Fikremariam Teshome Tekle

Assessment of Solar Energy Resources in Ethiopia

Modeling solar radiation and GIS-based multi-criteria analysis

Master's thesis in Natural Resources Management

Trondheim, May 2014

Supervisor: Ola Fredin

Norwegian University of Science and Technology
Faculty of Natural Sciences and Technology
Department of Geography

NTNU – Trondheim
Norwegian University of
Science and Technology

Abstract

The sun is an ultimate source of energy for life on earth, and hence the knowledge of solar radiation is essential for hydrological, climatological, biological modeling and utilization of renewable energy resources. Solar radiation can be measured from ground instruments at meteorological stations. Installations of instruments that directly measure global solar radiation are quite expensive, and thus spatial density of instruments is low. For instance, in Ethiopia there is only one Pyranometer, which is currently not functional. In addition, unlike rainfall and temperature, solar radiation cannot be interpolated for other areas with any degree of confidence from few sample measurements. This is mainly because the solar intensity is highly dependent on topography and surface features. Digital Elevation Models (DEMs) are important to derive these topographic characteristics that affect the amount of incoming solar radiation. Estimation of solar resources in a complex topography and inaccessible areas, where measurements are not available and/ or costly to measure over large areas from DEM is fast, cost effective and reliable. Ethiopia is located in the tropics and thus highly endowed with an abundance of solar energy. However, exploitation of solar energy is much underutilized and the energy sector is the least developed. The aim of this study is to calculate available solar energy resources and mapping the most suitable sites for large-scale PV installations in Ethiopia. The monthly and annual global solar radiations of Ethiopia were calculated from 30 meter resolution ASTER DEM using the ArcGIS solar radiation analysis tools. Solar radiation potential of Ethiopia ranges from 0.2 MWh/m^2/year in the lowlands (peripheral area) to 2.6 MWh/m^2/year in the central highlands. Large portion of Ethiopia receive solar radiation exceeding 1.8 MWh/m^2/year. Using GIS-based multi-criteria analysis, about 195 sites mainly in the eastern part of the country or 6000 km^2 in total, were selected as ideal locations for large-scale PV installations in Ethiopia. The selection process takes various topographic, economic, social and environmental factors into consideration. Selected sites could, if exploited properly, generate more than 65 GW, which is about 1/6 of electric power of all nuclear power plants in the world assuming 10 percent PV efficiency. Finally, a sensitivity analysis was performed to verify the selected sites. It is hoped that this study will promote investments in solar energy and encourage researchers for further studies in Ethiopia.

Keywords: Solar energy, Digital Elevation Models, Geographic Information Systems, Multi-Criteria Analysis

Acknowledgement

First and for most, I would like to express my deepest gratitude to Ola Fredin (Phd), who showed interest for supervision. His constructive comments and timely guidance during this study was very helpful. Without his support this thesis would not come to an end. My special thanks extend to my beloved family for their moral support and encouragement during my study. My darling '*Enat Yene'*, I thank you for your love and endless support. Finally, I like to acknowledge the Norwegian People and Government for their financial support to my MSc study in Norway.

Contents

Article manuscript

List of figures

List of tables

Abbreviations

Abbreviation	Explanation
a.m.s.l	above mean sea level
AHP	Analytic Hierarchy Process
ASTER	Advanced Space borne Thermal Emission and Reflection Radiometer
b.m.s.l	below mean sea level
cal/cm^2/day	calories per square centimeter per day
CIA	Central Intelligence Agency
CSA	Central Statistical Agency
DEM	Digital Elevation Models
EEPCo	Ethiopian Electric Power Corporation
ERA	Ethiopian Roads Authority
ERSDAC	Earth Remote Sensing Data Analysis Center
ESRI	Environmental System Research Institute
FAO	Food and Agricultural Organization
FDRE	Federal Democratic Republic of Ethiopia
GIS	Geographic Information Systems
GWh	Gigawatt hour
ha	hectare
km	kilometer
km^2	square kilometer
KWh	Kilowatt hour
LCCS	Land Cover Code Systems
LiDAR	Light Detection and Ranging
m	meter
MCA	Multi-Criteria Analysis
METI	Ministry of Economy, Trade, and Industry
mm	millimeter
MoIWE	Ministry of Irrigation, Water and Energy
MWh	Megawatt hour
NASA	National Aeronautic and Space Administration
NMA	National Meteorological Agency
NREL	National Renewable Energy Laboratory

NTNU	Norwegian University of Science and Technology
PV	Photovoltaic
SPSS	Statistical Packages for Social Sciences
SRTM	Shuttle Radar Topographic Mission
TWh	Terawatt hour
UN	United Nations
USA	United States of America
Wh/m^2	watt hours per square meter

Main introduction

Energy is the main economic artery of countries all over the world (Toman & Jemelkova, 2003), and can indeed be considered as the primary commodity in economy. The demand for energy is significantly increasing with increases in population and the rapid development of world's economy. As a result, the price of energy from conventional sources such as fossil fuels and nuclear power, are escalating through time. Nowadays, about 80 percent of the global primary energy demand is comes from fossil fuels, which are limited and thus become too expensive to exploit in the future (Uyan, 2013). While a majority of the world's energy supply is generated from fossil fuels, release of fossil carbon into the atmosphere has tremendous impact on the global climate. The production and consumption of energy from fossil fuels is by far the largest sources of greenhouse gases. Increasing greenhouse gas concentrations depletes the ozone layer, this in turn increase earth's average temperature, influence the patterns and amount of precipitations, reduce ice and snow cover, and raise sea level (Hardy, 2003). These changes will impact the food supply, water resources, the ecosystem, and earth's environment [6]. Renewable energy systems can help to mitigate global problems, such as climate change, poverty in developing world and insufficiency of energy supply from the conventional sources of energy (Kaygusuz, 2001; Šúri, Huld, Dunlop, & Hofierka, 2007).

Renewable energy refers to energy that is derived from resources that are constantly replaced in nature and usually less polluting the environment. Examples are biomass, sunlight, wind, water, geothermal heat and tide. They are abundant and environmental friendly sources of energy; and thus contribute to a sustainable economic development. To exploit the potential of renewable energy sources, there is a need to assess extent of available renewable energy sources spatially as well as temporally (Datta & Karakoti, 2010). The geographical dependency and dispersed nature of renewable energy generation impose questions that require specific location-dependent answers (Šúri, Huld, Dunlop, & Hofierka, 2007). Therefore, map based assessment of availability of renewable energy resources greatly contributes to increase investments and setting up effective renewable energy policies (Šúri, Huld, Dunlop, & Ossenbrink, 2007). Geographic Information Systems (GIS) helps in mapping available renewable resources on spatial and temporal scales and identifying ideal location for renewable energy development.

Solar energy is a vast and environmentally benign source of renewable energy, which is available everywhere on the planet however with significant variance. Solar radiation is the

key deriver of natural processes on the surface of the earth (Šúri, Huld, Dunlop, & Hofierka, 2007). Air and soil temperature and moisture, snow melting, photosynthesis, evapotranspiration processes are highly dependent on solar radiation (Tovar-Pescador et al., 2006). It plays a fundamental role in the energy exchange process between the atmosphere and the earth's surface. As a result, the knowledge of solar radiation is important for hydrological, climatological, biological modeling and applications (Martínez-Durbán et al., 2009). It also follows, that detailed understanding of the incoming solar radiation is vital for utilization of solar energy resources from solar panels at different scales.

Measurement of solar radiation at a wide spatial coverage is difficult because measuring instruments are very expensive. Unlike temperature and rainfall, solar radiation cannot be measured at sample meteorological stations and interpolated for the surrounding areas (Kumar, 2004).This is mainly because incoming solar radiation is highly dependent on topography and surface characteristics (Gastli & Charabi, 2010b; Li, 2013)[2]. Digital Elevation Models (DEMs) are useful to derive topographic characteristics such as elevation, slope, aspect and shadowing effects of neighboring terrain features, and thus helpful to estimate solar radiation particularly in a complex topography at a wide spatial coverage (Šúri, Cebecauer, & Skoczek, 2011).

The overall objective of this study is to assess solar energy resources of Ethiopia. In particular, available solar radiation potential was calculated from a high resolution DEM and ideal locations for large-scale Photovoltaic (PV) installations were selected using GIS-based Multi-Criteria Analysis.

The monthly and annual global solar radiations of Ethiopia were calculated from 30 m resolution ASTER Global DEM using Environmental System Research Institute (ESRI) ArcGIS solar radiation analysis tools. According to the GIS model, large portion of Ethiopia receives solar radiation exceeding 1.8 MWh/m^2/year. In total, 195 sites located in different regions at 0.5 percent of the total area of Ethiopia, were selected with aggregate electricity generation potential of 65 GW per year purely from solar radiation. The site selection takes various topographic, economic, social and environmental criteria into consideration. Finally, locations of the selected sites were verified through sensitivity analysis by altering the weight values of input criteria.

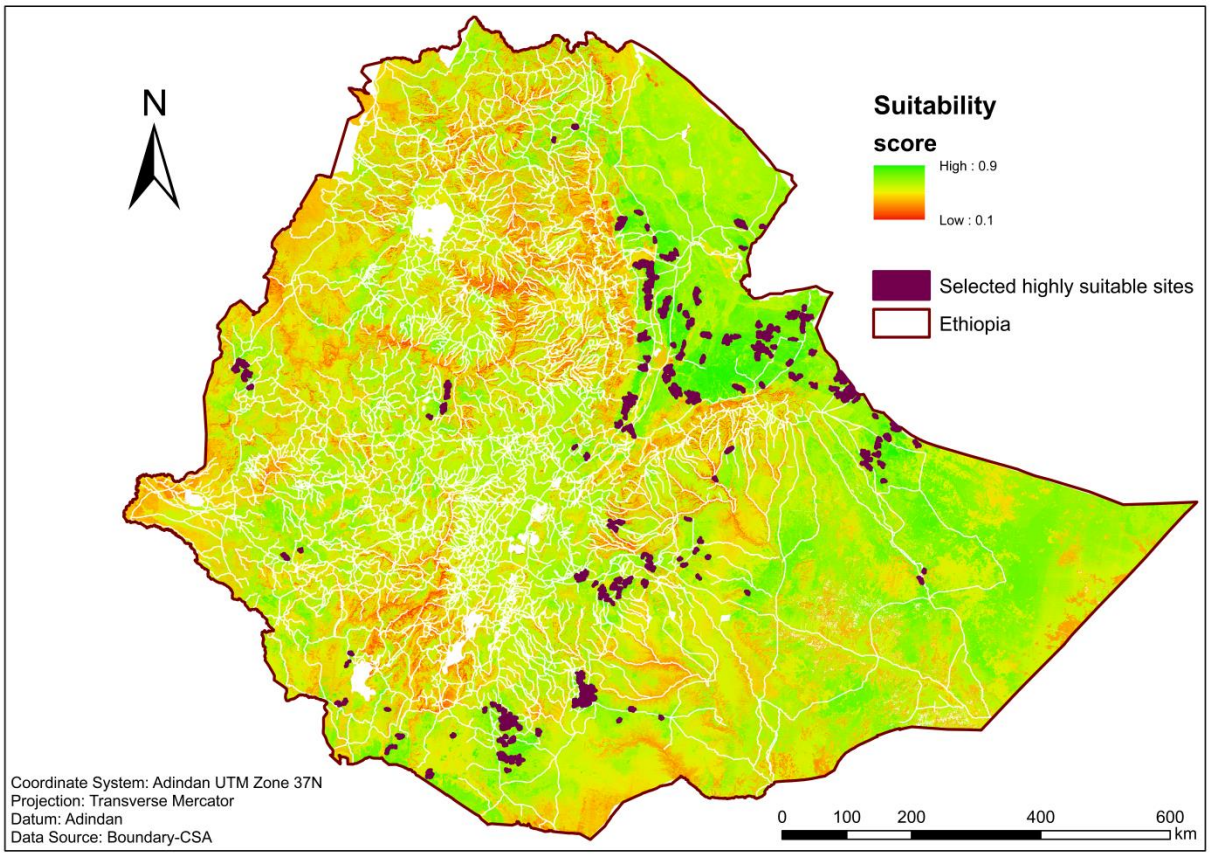

Figure 1*: Selected highly suitable sites for large-scale Photovoltaic installations in Ethiopia*

It is the aim to publish this study in an international journal such as *Solar Energy*, *Renewable Energy*, *Renewable and Sustainable Energy Reviews*, and thus to disseminate the results to a wider audience. Hence this thesis is submitted as article-based. It is hoped that at least one paper could be published titled *Assessment of Solar Energy Resources in Ethiopia: modeling solar radiation and GIS-based multi-criteria analysis*.

Article manuscript:

Assessment of Solar Energy Resources in Ethiopia: Modeling solar radiation and GIS-based multi-criteria analysis

1 Introduction

The sun is the ultimate source of energy for life on earth. Quantitatively, about 99.8 percent of energy at the surfaces of earth is derived from the Sun (Dickinson & Cheremisinoff, 1980). It is a powerhouse that sustains life on the earth surface. Solar energy is vast, free, clean and renewable power source that is available everywhere on the planet. However, the intensity of solar radiation reaching the surface of the earth shows considerable spatial and temporal variation at the local and on a global scale.

Solar radiation is a critical driver of evapotranspiration, surface and air temperatures, wind, growth and activity of plants and animals and other major processes on the earth surface (Kumar, Skidmore, & Knowles, 1997). It plays a major role in the energy exchange process between the atmosphere and earth's surface. As a result, the knowledge of solar radiation is important for hydrological, climatological, biological modeling and applications as well as utilization of renewable energy resources (Martínez-Durbán et al., 2009).

Solar power generation is a promising source of renewable energy and could alleviate global problems such as climate change, poverty in developing world and insufficient security of energy in the future (Šúri, Huld, Dunlop, & Hofierka, 2007). Thus, it contributes to a sustainable development of a region. However, in developing world the exploitation of solar energy is at a very low level.

The development of solar energy requires accurate estimation of the available solar energy resources and suitable sites for solar photovoltaic (PV) installations. The generation and distribution of solar energy is highly dependent on the geographical location and topography. Accurate knowledge of the available solar energy resource is very important for the design of any solar-based energy system. This knowledge can significantly contribute to better siting and economic assessment of the new installations, monitoring of their performance and forecasting of delivered energy (Šúri, Huld, Dunlop, & Hofierka, 2007).

Solar radiation can be measured from ground meteorological stations. The values measured from geographically dispersed stations can in theory be interpolated to generate a continuous solar map for the surrounding region (Li, 2013). However, intensity of solar radiation is highly dependent on topography and surface features. As a result, unlike rainfall and temperature that can be measured at a few locations and interpolated, solar radiation cannot be interpolated to a high degree of confidence (Kumar, 2004). Interpolation provides reasonable estimates in homogeneous terrain with uniform climatologic characteristics but in areas with

considerable topographic relief these estimates become unreliable (Tovar-Pescador et al., 2006). Installations of instruments that directly measure global solar radiation such as Pyranometers in various meteorological stations are quite expensive. As a result, in developing countries there are very few instruments for direct global solar radiation measurement. For instance, in Ethiopia there is only one Pyranometer which is currently not functional (Mekonnen, 2007). In most cases, meteorological data are heterogeneously located and they do not represent spatial and vertical variability of solar radiation adequately (Šúri, Huld, Dunlop, & Hofierka, 2007).

In complex topography, data interpolation is not adequate and reliable modeling of solar radiation is important, since intensity is highly dependent on elevation, slope, aspect and shadowing effects of neighboring terrain features (Bosch, Batlles, Zarzalejo, & López, 2010; Kumar, Skidmore, & Knowles, 1997). At the local scale, topography is the most important factor that determines the distribution of solar radiation on the surface (Martínez-Durbán et al., 2009; Tovar-Pescador et al., 2006). Digital Elevation Models (DEMs) are very helpful to derive these important topographic characteristics that affect the amount of incoming solar radiation. Relatively high resolution DEMs, for instance derived from Shuttle Radar Topographic Mission (SRTM), is very important in order to improve knowledge of solar energy resources on a regional scale (Šúri, Huld, Dunlop, & Ossenbrink, 2007). Therefore, estimation of solar energy resources in a complex topography on a wide spatial coverage from DEM is fast, cost effective and reliable. Moreover, the solar radiation map derived from DEM can be integrated with other data from various sources within Geographic Information Systems (GIS) to identify suitable sites for large-scale PV installations, and reduce risk and cost of potentially large energy investments. However, the estimation quality depends on DEM resolution and accuracy. Ethiopia is located in the tropics and thus highly endowed with an abundance solar energy. In fact, '13 months of sunshine' is the motto of Federal Democratic Republic of Ethiopian (FDRE) Ministry of Culture and Tourism. But the energy sector of Ethiopia is the least developed in the world and highly dependent on traditional sources of energy such as wood, crop residuals and animal waste. According to CIA, the electricity consumption per capita of Ethiopia in 2012 was 36.8 KWh per person, which is very low even in African standards [6]. Ethiopia is a mountainous country, where more than 46 percent of the total land mass is above 1,500 meter a.m.s.l. This highland ecosystem supports 80 percent of the total human population of the country (Tadesse & Belay, 2004).

Therefore, calculation of solar radiation from high resolution DEM using ArcGIS is a promising path to assess the solar energy potential of the country.

The aim of this study is to assess solar energy resources in Ethiopia based on high resolution DEMs using ArcGIS tools. Furthermore, optimal sites for extensive PV installations is calculated based on solar energy potential, population density, terrain, land use and several other factors. By doing this it is hoped that discussions can be initiated on using renewable solar power in general and in Ethiopia in particular.

2 Previous work

Related studies were conducted in different parts of the world using different approaches to calculate solar radiation potential and select ideal sites for PV installations. I have presented the following eight studies conducted at different scales from developing and developed countries.

Mekonnen (2007) has applied physical and empirical models with inputs of various meteorological data to predict the monthly average global radiation in Ethiopia for 17 stations. The models used in his analysis are the Simple Model of Atmospheric Radiative Transfer of Sunshine (SMARTS) and Vapor Pressure Radiation Model (VP-RAD). Maximum and minimum temperature, relative humidity, precipitation and surface pressure are some of the data used in this study. The monthly average results for Ethiopia, which ranges from 19.5 MJ m^{-2} day^{-1} to 20 MJ m^{-2} day^{-1} are observed from the SMARTS model prediction for the 17 stations. The VPRAD model is less accurate for global radiation predictions in Ethiopia. He concluded that Ethiopia is characterized on average, by relatively high daily global irradiance rates and high percentage of clear days.

Datta and Karakoti (2010) have mapped the solar potential in North-West regions of India based on global, diffuse, and direct solar radiation, which provides an estimate of potential sites for solar power generation applying GIS. They have demonstrated that importance of GIS for mapping both spatial and temporal variability of solar energy supply and demand.

Gastli and Charabi (2010) have developed the first geographical mapping models to locate the most appropriate sites for different Concentrated Solar Power (CSP) technologies in Oman. They calculated the global distribution of solar radiation within the boundaries of Oman, based on a DEM with 3 km resolution using ArcGIS Solar Radiation Analysis tools. Only slope analysis was considered in calculating the yearly electricity generation potential for different Concentrated Solar Power (CSP) technologies, and thus only 10 percent of the land of Oman with a slope of less than 1 percent was considered as exploitable land. The total calculated potential of yearly electricity generation would be about 7.6 million GWh, which is many times higher than the current generation supply in Oman which was about 11,189 GWh in 2007. The results obtained show very high potential of solar radiation over all the lands of Oman.

Janke (2010) has identified areas that are suitable for wind and solar farms using multi-criteria GIS modeling techniques in Colorado, USA. Renewable potential (NREL wind speed

measurements at 50 m above the ground and NREL annual insolation data), land cover, population density, federal lands, and distance to roads, transmission lines, and cities were considered for finding suitable locations. The GIS model indicates that ideal areas for wind and solar farm developments are located in northeastern and northwestern part of the state and east of Denver at 41,850 km^2 and 191 km^2, respectively. The GIS model is very well equipped at detecting regional renewable energy facilities that are capable of supporting large urban populations, he concludes.

Bhuiyan (2013) estimated empirically global, diffuse and direct solar radiation on a horizontal surface for ten stations equally distributed all over Bangladesh as well as predicted correlations for them. For this study, meteorological data (temperature and sunshine hour to predict global radiation; relative humidity and atmospheric water to estimate diffuse radiation; and sunshine duration to estimate direct radiation) for the years 1980 to 2007 was used. The global radiation in Bangladesh is found to be highest in the months of April and May and lowest in the months of November and December in all the districts. He concluded that Bangladesh is endowed with sufficient solar radiation throughout the year and correlations proposed for Bangladesh in this study can be used in future for estimation of solar radiations if the meteorological data are available.

Charabi and Gastli (2011) have assessed solar energy resources in Oman, in particular GIS-based spatial multi-criteria evaluation approach. In particular the FLOWA module was used to assess land suitability for large PV farms installations. The tool used applies fuzzy quantifiers within ArcGIS environment allowing the integration of a multi-criteria decision analysis. The overlay results obtained from the output maps showed that 0.5 percent of the total land area demonstrate a high suitability level. It was also found that the CPV technology provides very high technical potential for implementing large solar plants. In fact, if all highly suitable land is completely exploited for CPV implementation, it can produce almost 45.5 times the present total power demand in Oman.

Li (2013) has employed GIS and remote sensing techniques for determining the optimal sites for solar panel installation at micro and macro-scales: building rooftop installations at the University of Waterloo main campus and ground-mounted installation in the City of Waterloo, Canada, respectively. Light Detection and Ranging (LiDAR) and DEMs were used to derive accumulated solar radiation energy under clear-sky and overcast conditions using ArcGIS software. Optimal ground-mounted solar panel installation sites were determined using a multi-criteria analysis approach that considered various environmental and

socioeconomic factors. He identified building roofs with a southern exposure without obstructions and four potential sites close to the periphery of the city at micro and macro scales. Moreover, Li conducted a questionnaire survey of three Ontario solar companies to obtain information about how solar companies in Ontario select potential sites for solar PV installation. Finally, a feasibility assessment was performed with ground truth information to verify selected sites.

Uyan (2013) has determined suitable site selection for solar farms by using GIS and Analytical Hierarchy Process (AHP) in Karapinar region, Turkey. He considered the quality of terrain, local weathering factors, proximity to high transmission capacity lines, agricultural facilities and environmental conservation issues in the selection process. He found that 13.92 percent of the study area (840.07 km^2) as highly suitable for solar farms.

Based on these pioneering studies it is concluded that GIS analysis, where potential incoming solar radiation is calculated using a relatively high resolution DEM, together with considerations of physiographic and socioeconomic factors would be the most suitable to map solar power potential in a relatively large country such as Ethiopia.

3 Materials and methods

3.1 The study area

Ethiopia is located between latitude 3° and 15° North and longitude 33° and 48° East in the north eastern Africa, sometimes also known as Horn of Africa (Fig.1). It shares about 5328 km boundary line with Eritrea in the north, Djibouti in the east, Somalia in the south east, Kenya in the south, South Sudan and Sudan in the west. With over 80 million human inhabitants, Ethiopia is the second most populous country in Africa [3]. The total area of the country is 1.1 million km^2 [4].

Ethiopia is a country of great geographical diversity. Located within the tropics, its physical conditions and variations in altitude have resulted in a great range of terrain, climate, soil, flora and fauna. The geography also determines the population settlement patterns of the country. Ethiopia has high and rugged mountains, flat-topped plateaus, deep gorges, incised river valleys and vast rolling plains. Its altitude ranges from the highest peak at Ras Dashen in the north (4620 meter a.m.s.l) down to the Dallol (also known as the Danakil) depression in the east, approximately 148 meter b.m.s.l [4]. The Great Rift Valley separates the western and the eastern highlands; and these highlands gradually descend to the lowland areas in the east, west, and south of the country [4]. Much of the country thus consists of high plateau and mountain ranges, which are dissected by numerous streams and rivers. Among the biggest river basins are Blue Nile, Awash, Baro, Omo, Tekkeze, Wabe Shebelle and Genale.

Ethiopian climate varies according to the different topographical regions. The central plateau has a favorable climate with minimal seasonal temperature variation. In contrary, temperature variations in the lowlands are much greater. There are two distinct seasons in Ethiopia, the dry season which is for the most part from October to May and rainy season from June to September (Mekonnen, 2007). The mean annual temperature ranges from 20^{o}C in the central plateau to 30^{o}C in the lowlands. Heavy rainfall occurs in most of the country during June, July and August and smaller rains in February and March. The mean annual rainfall varies between 200 mm in the east and north to 2000 mm on the central highlands.

Ethiopia is an ecologically diverse country, ranging from the deserts along the eastern border to the tropical forests in the south to extensive Afro-mountain in the northern and southwestern parts.

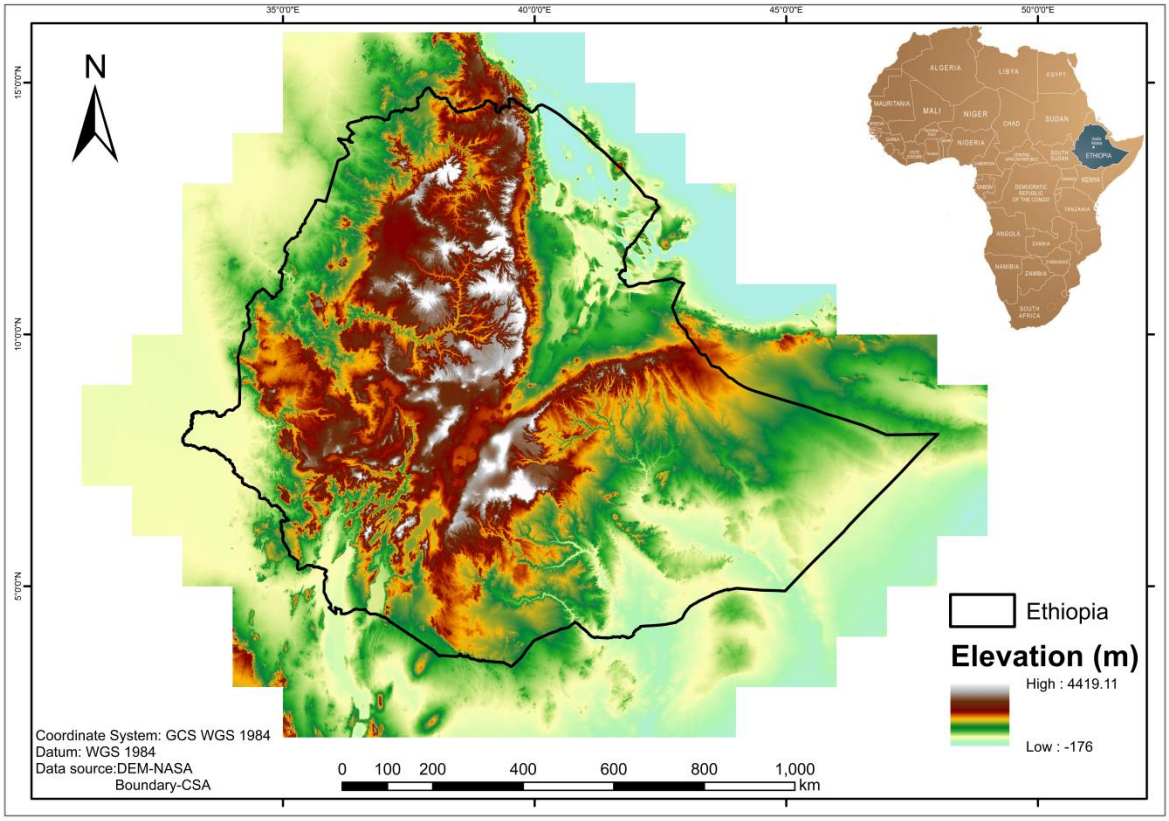

Figure 2: Digital Elevation Model and location map of the study area

3.2 Data sources and processing

Various spatial and non-spatial datasets were obtained from different organizations and processed using multiple GIS tools for mapping and analysis purposes. A relatively high resolution, accurate and geo-referenced DEM dataset is the most important input to calculate solar radiation using ArcGIS solar radiation analysis tools. DEMs were needed to model important topographic characteristics such as elevation above sea level, slope inclination, terrain orientation and shadowing effects of the neighboring terrain features that affect the amount of incoming solar radiation. For this study DEMs were derived from the Advanced Space-borne Thermal Emission and Reflection Radiometer (ASTER) global DEMs version 2 [9]. The Ministry of Economy, Trade, and Industry (METI) Earth Remote Sensing Data Analysis Center (ERSDAC) in Japan and the National Aeronautic and Space Administration (NASA) Earth Observing System (EOS) Data Information System (DIS) Land Processes (LP) Distributed Active Archive Center (DAAC) in the United States jointly released a second version of the ASTER Global DEM without charge as a contribution to the Global Earth Observing System in mid-October, 2011 (P. Li et al., 2012). ASTER DEM is distributed as 1° x 1° tiles, and therefore 175 tiles that cover about 2.1 million km^2, which contained 1.1

million km^2 study area, were downloaded from NASA thus allowing the horizon effects on the estimated solar radiation to be taken into account properly. The ASTER Global DEM version 2 has additional scenes to reduce artifacts, higher horizontal resolution using smaller correlation kernel and an improved water mask compared with the previous version. The ASTER Global DEMs obtained elevation data on a near-global scale to generate the most complete high-resolution digital topographic database of earth. Global DEMs data were released at a 1 arc-second (30 meter) resolution (Tachikawa, Hato, Kaku, & Iwasaki, 2011).

In order to evaluate the reliability of solar radiation values modeled from DEMs using the solar radiation analysis tools in ArcGIS, solar intensity data of ten stations in the study area were collected from National Meteorological Agency (NMA) of Ethiopia. The meteorological stations are Addis Ababa, Arba Minch, Bahir Dar, Kombolicha, Debre Tabor, Dedessa, Dire Dawa, Metehara, Nazreth and Welayita Sodo. The locations of these stations range from 930 meter a.m.s.l at Metehara to 2690 meter a.m.s.l at Debre Tabor. These stations have relatively complete and recent daily solar intensity recorded in $cal/cm^2/day$. Due to absence of Pyranometers in different parts of the country and recent solar intensity values measured using Actinographs, the daily solar intensities of these stations were thus recorded in 1990s from Actinographs by NMA. In Ethiopia the NMA is responsible for installing meteorological stations, collecting all meteorological data, archiving of meteorological and climatological data as well as providing meteorological services to all stakeholders [5]. It is also responsible for publishing and disseminates analyzed and interpreted meteorological data and meteorological forecasts. Figure 3 and table 1 show the location and the characteristics of the selected meteorological stations, respectively.

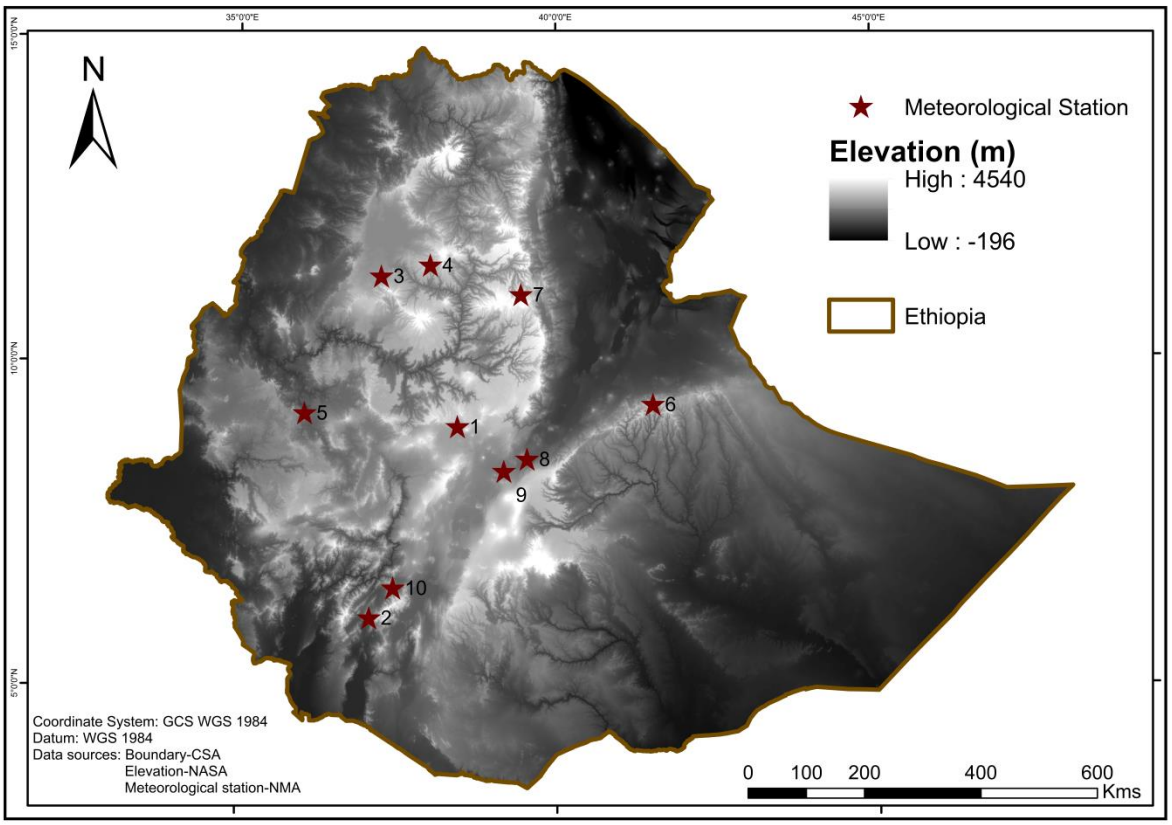

Figure 3: *Locations of selected meteorological stations*

Table 1: *Characteristics of selected meteorological stations*

Station Number	Station Name	Longitude (East)	Latitude (North)	Elevation (meter a.m.s.l)	Data Recording (year)
1	Addis Ababa	38.45	9.02	2408	1997
2	Arba Minch	37.08	6.05	1290	1995
3	Bahir Dar	37.25	11.36	1770	1996
4	Debre Tabor	38.02	11.53	2690	1995
5	Dedessa	36.06	9.23	1200	1990
6	Dire Dawa	41.51	9.36	1260	1997
7	Kombolcha	39.44	11.07	1903	1995
8	Metehara	39.54	8.52	930	1996
9	Nazreth	39.17	8.33	1622	1997
10	Welayita Sodo	37.45	6.51	1800	1997

In addition to solar radiation potential, selection of ideal sites for large-scale solar panel installations require other datasets such as land cover, existing road network, existing power transmission network, population density, and environmental protected areas. Land cover is important for natural resource assessment and management, environmental modeling and decision-making. A land cover map of the study area was obtained from Food and Agricultural Organization (FAO) of the United Nations [11]. This land cover database was provided as ESRI shape file (vector format) and is sourced from reprocessing the raster based Globcover database (regional version) [12]. It has been post-processed to generate a vector version at national extent with the Land Cover Code System (LCCS) regional legend (46 classes). Globcover is currently the most recent (2005) and finest resolution (300 meter) datasets on land cover globally. It was published in 2008 and intended for free public access [11].

Population density refers to number of persons per km^2. Population density map of the study area was mapped using an analogue map of Ethiopian Somali region and digital map of other regions and number of population per Woreda[1] obtained from the FDRE Central Statistical Agency (CSA) of Ethiopia. Population density mapping was thus performed through: a) scanning, geo-referencing and digitization of Ethiopian Somali region Woreda's boundary from the analogue map; b) merging with other region's Woreda map that are initially obtained in digital format; c) joining attribute data; and d) classification based on number of people per km^2 in the Woreda boundary.

Road and power transmission network maps of Ethiopia were also important for site selection, since existing infrastructure determine cost of the construction, transmission and maintenance (Janke, 2010). Digital road network map and analogue power transmission network maps were obtained from the FDRE Ethiopian Roads Authority (ERA) and the FDRE Ethiopian Electric Power Corporation (EEPCo) respectively. To perform GIS analysis the analogue map was scanned, geo-referenced, and finally digitized to get the digital copy of it. Maps of parks and environmental protected areas were obtained from the FDRE Environmental Protection Authority (EPA). In addition, lakes and river network map of Ethiopia were obtained from the FDRE Ministry of Irrigation, Water and Energy (MIWE) in digital format. All these datasets were used as criteria for siting large-scale solar panel installations. Type and source of data used in this study are summarized in the following table.

[1] Woreda or district: the second-level administrative divisions of Ethiopia. They are composed of Kebeles which are the smallest unit of local government.

Table 2: *Type and source of data used in the study*

Data	Source	Original Data	Data Year	Final Data	Final Resolution
ASTER Global Digital Elevation Models version 2	The US National Aeronautics and Space Administration (https://earthdata.nasa.gov/)	Raster	2011	Raster	30 m
Observed solar intensity	The FDRE National Meteorological Agency	Charts	1997	NA	NA
Land cover	Food and Agricultural Organazation of the UN (http://www.fao.org)	Digital, Polygon	2005	Raster	30 m
Population density (Woreda boundary & No. of population)	The FDRE Central Statistical Agency	Analogue& Digital, Polygon & Table	2007	Raster	30 m
Road network	The FDRE Ethiopian Roads Authority	Digital, Polyline	2007	Raster	30 m
Power transmission network	The FDRE Ethiopian Electric Power Corporation	Analogue, Polyline	2010	Raster	30 m
Rivers and Lakes	The FDRE Ministry of Water, Irrigation and Energy	Digital, Polyline and Polygon	2007	Raster	30 m
Environmentally Protected Areas	The FDRE Environmental Protection Authority	Digital, Polygon	2007	Raster	30 m
Boundary of Ethiopia	The FDRE Central Statistical Agency	Analogue, Polygon	2007	Vector	NA

3.3 Methods

Monthly and annual global solar radiation maps of Ethiopia were calculated from 30 meter resolution DEM, which subsequently used as criteria for suitable site selection. A GIS-based Multi-Criteria Analysis (MCA) approach was adopted to select sites for large-scale PV solar farms in Ethiopia. This section discusses the methodology of the study in detail.

3.3.1 Modeling solar radiation

Solar radiation reaching the surface of the earth shows considerable spatial and temporal variation at the local and on a global scale. On a global scale the major controlling factors are the latitude, distance from the sun, and time of year [2]. Whereas at the local scale major sources of spatial variation are elevation above sea level, surface inclination, surface orientation, and shadowing effects of neighboring terrain features. These topographic parameters can be modeled and derived from high resolution DEMs. As a result, the most important input to calculate solar radiation was an accurate, geo-referenced and high resolution DEM dataset. As mentioned earlier, for this study 30 meter resolution DEMs were derived from ASTER Global DEM version 2.

In the last decade different individuals and institutions have developed several GIS-based radiation models for calculating incoming radiation on global areas represented by DEMs (Tabik, Villegas, Zapata, & Romero, 2012). Solar Analyst and r.sun are some of the tools developed under ArcGIS and GRASS GIS respectively used to calculate direct and diffuse

radiation maps over smaller areas. As this study deals with calculation of solar radiation covering comparably much larger areas using high resolution DEMs, the solar radiation tools found in ArcGIS and developed by ESRI, was found to be a suitable tool for this study. The solar radiation analysis tools allows mapping and analysis the effects of sun over a geographic area for specific time periods (Charabi & Gastli, 2010; Gastli & Charabi, 2010b)[1]. It calculates insolation based on methods from the hemispherical viewshed algorithm developed by (Rich, Dubayah, Hetrick, & Saving, 1994). The solar radiation tool accounts for atmospheric effects, site latitude and elevation, steepness (slope) and compass direction (aspect), daily and seasonal shifts of the sun angle, and effects of shadows cast by surrounding topography (Li, 2013) [2]. The output radiation raster is floating-point type, have units of watt hours per square meter (Wh/m^2) and could be easily integrated with other GIS data for further applications.

Due to earth's atmosphere, all the radiation, which comes from the sun will not directly reach earth's surface. It usually is attenuated by absorption, scattering and reflection before reaching the land surface. The total (global) radiation at the surface of the earth is the sum of direct solar radiation, scattered (diffuse) solar radiation, as well as reflected solar radiation (Kumar et al., 1997). Direct (beam) radiation is the largest and the most important component of global radiation and diffuse radiation is the second largest component. Reflected radiation generally constitutes only a small proportion of total radiation, except for locations surrounded by highly reflective surfaces such as areas with extensive snow cover [2]. Calculations of radiation using ArcGIS solar radiation analysis tool do not include reflected radiation in the calculation of total radiation. As a result, the total radiation obtained from ArcGIS is the sum of the direct and diffuse radiation. Since snow cover and other reflective surface are low in the study area, it is assumed that absence of reflected radiation does not affect the calculated output to a significant degree. Moreover, ArcGIS solar radiation analysis tool do not consider the effects of clouds in the solar radiation calculation.

With large DEM dataset, the insolation would differ significantly at different latitudes (greater than 1 degree). To analyze broader geographic regions like in this study, it is necessary to divide the study area into zones with different latitudes. Since the study area is situated between latitude 3° and 15° north, it is divided into 13 zones with different latitudes. In addition to these major zones, minor zones (latitude 0.4° DEM tile) that share common area from two consecutive major zones were created to properly take in to account the effect of neighboring topography in the calculation (figure 4).

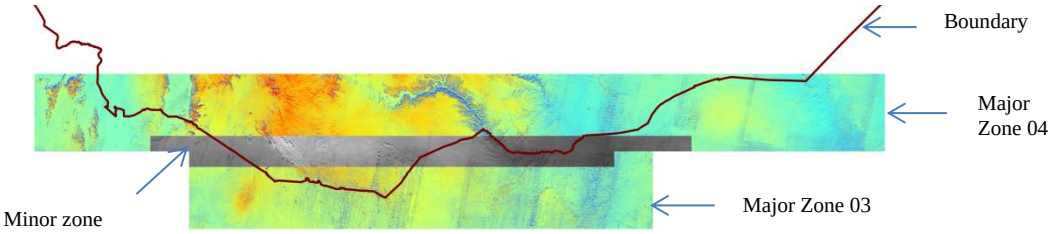

Figure 4: *Major and minor zones*

Since solar radiation can be greatly affected by topography and surface features, a key component of the calculation algorithm requires the generation of an upward-looking hemispherical viewshed for every location in the DEM [2]. The viewshed is a raster representation of the entire sky that is visible or obstructed when viewed from a particular location. In addition, it needs the sun's position in the sky across a period of time (sunmap) and the sectors of the sky that influence the amount of incoming solar radiation (skymap) [1]. The solar radiation tools calculations essentially involves four steps:

1. Calculation of an upward-looking hemispherical viewshed based on topography.
2. Overlay of the viewshed on a direct sunmap to estimate direct radiation.
3. Overlay of the viewshed on a diffuse skymap to estimate diffuse radiation.
4. Repeating the process for every location of interest to produce an insolation map.

In addition to DEM resolution, the accuracy and processing time of insolation calculations depend on sky size and time interval. Sky size is the resolution of the viewshed, sky map, and sun map rasters which are used in the radiation calculations (units: cells per side). Bigger sky size and smaller time interval increases accuracy but also increases calculation time considerably (Gastli & Charabi, 2010b; Li, 2013)[2]. As a result, in this study sky size of 2,800, which is recommended to calculate insolation for a location at the equator and the default 14 days and 0.5 hour interval were used. To increase calculation accuracy the number of calculation direction was also set to 32, which is adequate for complex topography [2]. Appropriate z factor was assigned to adjust the units of measure for z units as they are different from the ground x,y units of the input DEM raster.

Solar radiation of whole year with monthly interval was calculated for each major and minor zone. Insolation calculation from large and relatively higher resolution DEMs are time consuming and require high speed computers. For this study the calculation of annual and monthly global solar radiation for the whole Ethiopia takes about three months from October, 2013 to January, 2014 using multiple high speed computers running in parallel, processing

one zone each at the department of Geography GIS lab, NTNU. Finally, using the ArcGIS mosaic tool annual and monthly solar radiation for each month in a year was calculated for the whole Ethiopia. This approach has the advantage of providing fast, cost effective and reliable results on a wide spatial coverage.

3.3.2 Comparison between observed and modeled solar radiation

In order to compare ground recorded global solar radiation with GIS-modeled solar radiation, monthly solar radiations of the ten sample stations were also calculated using the ArcGIS point solar radiation tool. Point solar radiation tool calculate incoming solar radiation for specific locations in a point feature or location table from DEM surface. To compute the correlation, mean monthly radiation value have been used for every month of the year for all meteorological stations, providing 120 values. 26 values were excluded from the final computation due to incompleteness. Finally, simple regression analysis in SPSS was performed to show the correlation between 94 observational data and GIS-modeled solar radiation.

3.3.3 GIS-based Multi-Criteria Analysis

Site selection process for large-scale solar panel installation involves various social, technological, environmental and economic aspects. GIS-based Multi-Criteria Analysis (GIS-MCA) provide a flexible tool that is able to handle and bring together wide range of variables assessed in different ways and thus offer useful assistance to the decision maker in pointing at suitable locations (Taha & Daim, 2013). It is a process that transforms and combines spatial data and value judgments to obtain information for decision making (Malczewski, 1999).

In order to select best sites for large-scale PV solar farms in Ethiopia, I have used the following six steps. The initial step is set the goal or problem definition. In this study the aim of GIS-based MCA is to produce a map showing ideal sites for large-scale PV installations in Ethiopia. The objective was specific, measurable and attainable. The second step was determining factors/ criteria that are important for large-scale solar panel installations. The factors used for site selection process for a particular land use should be selected by the experts and researchers of that particular land use. Based on literatures and related studies conducted in different areas (Charabi & Gastli, 2011; Gastli & Charabi, 2010a; Janke, 2010; Li, 2013; Turney & Fthenakis, 2011; Uyan, 2013) solar radiation potential, land cover, population density, proximity to existing road networks, proximity to existing power transmission networks, and distance to water sources as well as slope and aspect were selected

as factors that are important for the large-scale PV solar farms site selection process in Ethiopia. These datasets were collected from various sources and processed using ArcGIS software for MCA. These are not the only factors that are important to select sites for large-scale PV installations. Other datasets such as wind speed map, map of cultural heritage sites, and future land use map at the study area, which needs to be considered were unavailable during this study.

The third step was standardizing each factors/ criterion scores. It is important to set the suitability values of the factors to a common scale to make comparisons possible. Therefore, all input datasets were changed into a raster at 30 meter resolution and to a common measurement scale using the Conversion and Reclassify tools found in ArcGIS respectively. They were reclassified from 1 to 5; where 5 represent the most suitable conditions for large-scale PV installations. For instance, the solar radiation raster was reclassified from 1 to 5; where 5 represent the highest solar radiation value and thus the most favorable condition for solar panel installation.

Land cover data set consisted of 20 land cover classifications identified within study area. The polygons representing different land cover types were converted into a raster and finally categorized into five classes according to their suitability for large-scale PV solar farms. Suitable land cover includes bare areas, grassland, and savannas. Permanently unsuitable land cover contained forest, urban areas, water bodies, flooded land. Crop lands, closed grass land, sparse vegetation, shrub lands were not as highly suitable and categorized as marginally suitable land cover. Table 3 below show classification of different land cover types identified in the study area based on their suitability to solar panel installation.

Population density map was converted into a raster with a 30 m resolution and standardized from 1 to 5; where 5 indicate the lowest population density and hence the most ideal condition for large-scale PV installations. A Euclidian distance raster was calculated at a 30 m resolution for the existing road and power transmission networks as well as distance to water source. Then, the Euclidean distance raster was reclassified from 1 to 5; where 1 represent faraway locations and thus the least desirable areas while 5 represent locations very closer to existing roads and transmission lines and water sources, and thus the most ideal location for solar energy development.

Slope and aspect were other factors that determine suitability of a given land for PV solar farms. These data were derived from 30 meter resolution ASTER DEM using the ArcGIS spatial analyst tools and reclassified from 1 to 5 based on their suitability to solar panels

installations. Gentle slope areas facing south, south east and south west directions are the most desirable location for large-scale solar panel installations. Because southerly facing land surfaces have the higher exposure to sun the northern hemisphere (Gastli & Charabi, 2010a; Li, 2013) [15].

Table 3: *Classification of various land covers based on their suitability to solar panel installation*

Highly suitable		Moderately suitable		Marginally suitable		Not suitable		Non suitable	
LCCS	**Description**	**LCCS**	**Description**	**LCCS**	**Description**	**LCCS**	**Description**	**LCCS**	**Description**
151	Sparse (<15%) grassland	120	Mosaic grassland (50-70%) / forest or shrubland (20-50%)	14	Rainfed croplands	110	Mosaic forest or shrubland (50-70%) / grassland (20-50%)	40	Closed to open (>15%) broadleaved evergreen or semi-deciduous forest (>5m)
200	Bare areas	140	Closed to open (>15%) herbaceous vegetation (grassland, savannas or lichens/mosses)	20	Mosaic cropland (50-70%) / vegetation (grassland/ shrubland/forest) (20-50%)	130	Closed to open (>15%) (broadleaved or needleleaved, evergreen or deciduous) shrubland (<5m)	41	Closed (>40%) broadleaved evergreen and/or semi-deciduous forest (>5m)
201	Consolidated bare areas (hardpans, gravels, bare rock, stones, boulders)	150	Sparse (<15%) vegetation	30	Mosaic vegetation (grassland/ shrubland/ forest) (50-70%) / cropland (20-50%)	162	Closed to open broadleaved forest on temporarily flooded land - Fresh water	60	Open (15-40%) broadleaved deciduous forest/woodland (>5m)
202	Non-consolidated bare areas (sandy desert)			141	Closed (>40%) grassland	180	Closed to open (>15%) grassland or woody vegetation on regularly flooded or waterlogged soil - Fresh, brackish or saline water	190	Artificial surfaces and associated areas (Urban areas >50%)
								210	Water bodies

The fourth step was defining weights for each criterion based on its importance for the large-scale PV installations. Several methods are available to determine the weight and in this study the Analytical Hierarchy Process (AHP) method was adopted to assign weight for each factor (Saaty, 1980). A pairwise comparison matrix was constructed, where each criterion was compared with the other criteria, relative to its importance, on a scale from 1 to 9 as shown in table 4. An Eigen-vector or weight was calculated for each criterion and used to derive a consistency ratio of the pairwise comparisons. 0.25, 0.23, 0.05, 0.11, 0.11, 0.04, 0.02, and 0.19 was obtained as a weight value for the solar radiation potential, land cover, distance to power transmission network, aspect, slope, distance to water source and population density respectively with 6.4 percent consistency ratio. According to Saati, who developed AHP, consistency ratio of less than 10 percent shows consistent comparison between the criteria and it was deemed as acceptable (Saaty, 1980).

Step five was to aggregate the criteria using weighted linear combination and apply it in the ArcGIS raster calculator. The output raster was converted to polygons and small polygons with less than 2.5km^2 were filtered out, since this is the smallest acreage required to produce

100 MW electricity from PV solar farms (Charabi & Gastli, 2010). Verification of results was the last step and usually assessed by ground truth verification and sensitivity analysis.

Table 4: *Pairwise Comparison Matrix*

Criterion	Solar Radiation	Land Cover	Distance to Grid	Aspect	Slope	Distance to Road	Distance to Water	Population Density	Weight (%)
Solar Radiation	1	1	7	2	3	7	9	2	**25.13**
Land Cover	1	1	5	3	3	7	9	1	**23.17**
Distance to Grid	0.14	0.20	1	0.20	0.20	2	6	0.33	**5.04**
Aspect	0.5	0.33	5	1	1	2	9	0.5	**11.44**
Slope	0.33	0.33	5	1	1	2	9	0.33	**10.50**
Distance to Road	0.14	0.14	0.5	0.5	0.5	1	3	0.14	**3.77**
Distance to Water	0.11	0.11	0.17	0.11	0.11	0.33	1	0.11	**1.68**
Population Density	0.5	1	3	2	3	7	9	1	**19.28**

Due to size of the study area, shortage of time, and unpracticality of field surveys only sensitivity analysis was performed by weight value of the factors to assess the reliability of the output.

4 Results

To select suitable sites for large-scale PV solar farms in Ethiopia, solar radiation potential of the country should be assessed first. A solar radiation map was derived from high resolution DEM employing ArcGIS solar radiation analysis tool, showing the monthly and annual solar radiation potential of the country. GIS-based Multi-Criteria Analysis (GIS-MCA) was applied to map suitable sites for large-scale PV solar farms in Ethiopia. In addition to solar radiation potential land cover, population density, infrastructure and topographic characteristics of the study area were taken into account properly in the site selection process. This section shows the spatial and temporal variation of solar radiation and optimal locations for large scale solar energy development in Ethiopia.

4.1 The spatial distribution and temporal variation of solar radiation

The daily, monthly and annual global solar radiation of Ethiopia was calculated from 30 m resolution ASTER DEM using the ArcGIS solar radiation analysis tools. Figure 5 below shows the annual distribution of global solar radiation of Ethiopia per square meter. According to this analysis, solar radiation potential of Ethiopia ranges from 0.2 MWh/m^2/year in the lowlands (peripheral area) to 2.6 MWh/m^2/year in the central highlands. The radiation increases with increasing altitude above sea level. This is mainly because of a pronounced increase of direct irradiance (Blumthaler, Ambach, & Ellinger, 1997). Due to their relative location, size, and elevation regions of Oromia, Amhara, west Tigray and north Southern Nations Nationalities and Peoples received the higher global solar radiation compared to regions located in the lowlands and periphery parts of the country. Larger portion of the country received solar radiation exceeding 1.8 MWh/m^2/year. The geographical location of Ethiopia, close to the equator, clearly plays an important role.

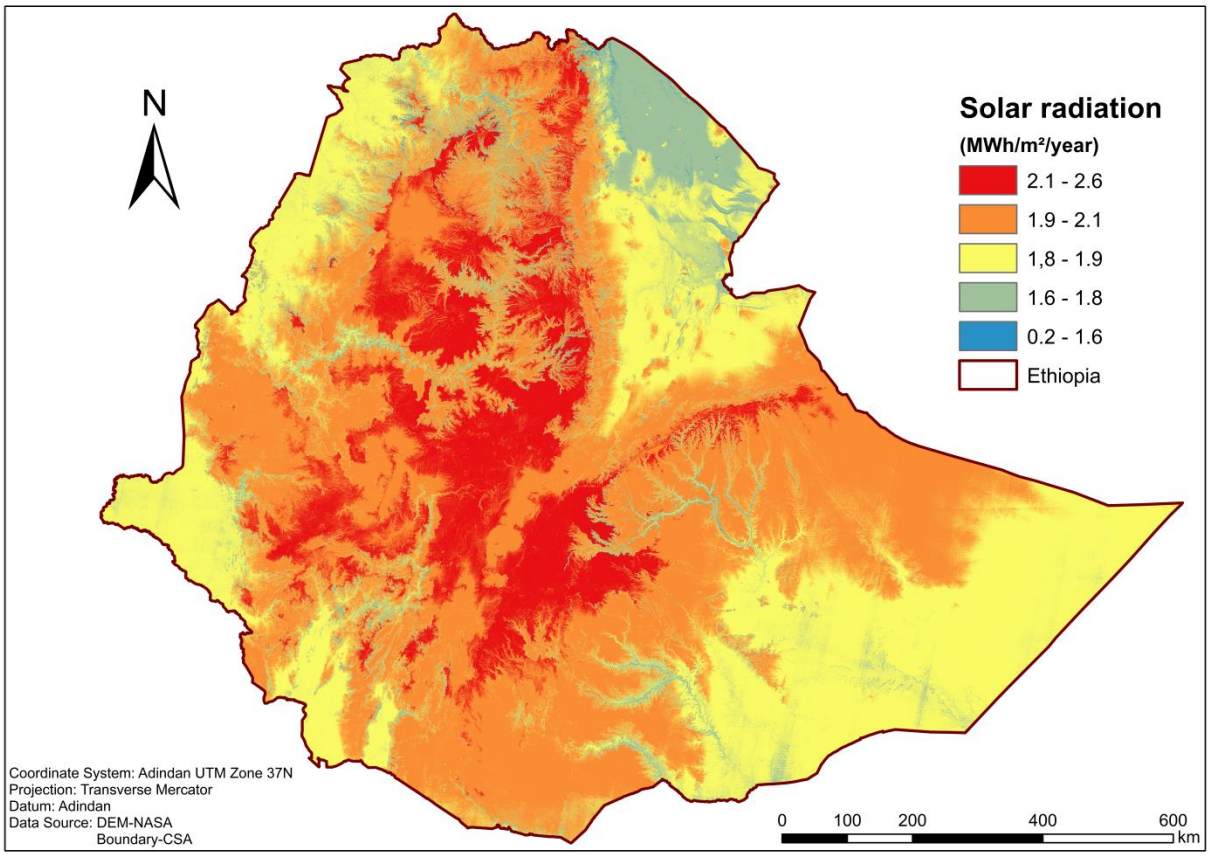

Figure 5: *Distribution map of annual global solar radiation in Ethiopia*

Furthermore, global solar radiation of the country showed variation through months of the year. Table 5 and figure 6 shows the minimum, the maximum and the mean global solar radiation of each month in a year. November, December, January and February received the lowest mean solar radiation, while May, July, August and September received the highest mean global solar radiation in a year. Since Ethiopia is situated in the Northern hemisphere the winter and the summer solstice is in December and June, respectively. In summer, due to longer duration of sunlight and perpendicular angle of the sun rays reaching the surface in the Northern hemisphere, solar radiation received in this hemisphere reaches its maximum. In contrary, during winter the Northern hemispheres receive lower radiation as a result of shorter duration of sunlight and oblique angle of the sun rays reaching the ground.

Table 4: *Temporal variation of monthly global solar radiation in Ethiopia*

Global solar radiation (Wh/m^2/month)	Month	January	February	March	April	May	June	July	August	September	October	November	December
	Min	1,930	2,148	3,646	15,348	6,961	3,286	4,026	11,533	6,624	2,376	1,912	1,858
	Max	221,940	207,232	236,328	238,981	255,147	250,390	257,094	249,714	239,322	224,323	216,207	219,516
	Mean	136,288	138,439	170,906	172,893	176,442	167,735	175,074	178,741	174,338	153,691	135,489	130,485
	Std dev.	16,161	13,212	12,501	11,899	14,233	14,906	14,788	12,792	12,143	13,549	15,351	16,523

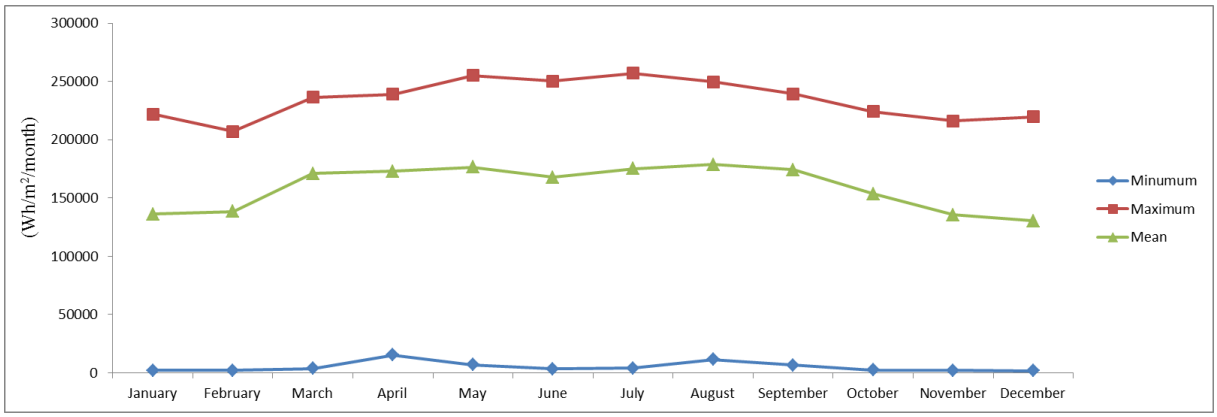

Figure 6: *Temporal variation of monthly global solar radiation in Ethiopia*

4.2 Comparison between observed and modeled solar radiation

Correlation between recorded and modelled global monthly solar radiation values of ten meteorological stations obtained from Actinograph and ArcGIS respectively were calculated using Statistical Packages for Social Sciences (SPSS). Measurement unit for observed data is cal/cm^2 and for ArcGIS data it is Wh/m^2. The R^2 value of 0.65 shows that there is a correlation between observed and modeled values.

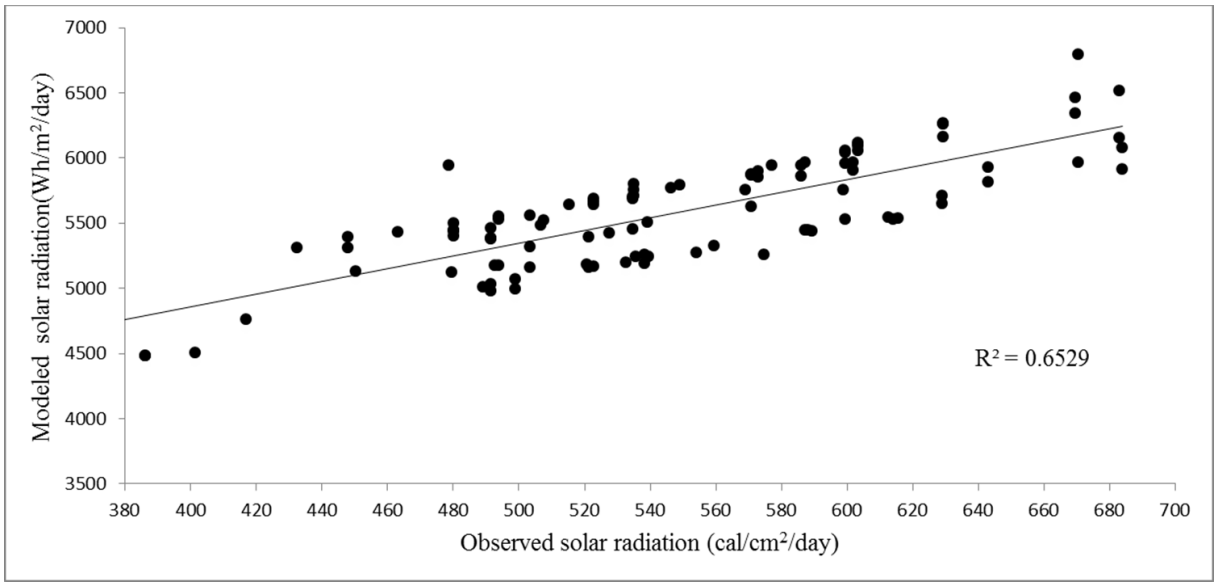

Figure 7: *The correlation between the observed and the modeled solar radiation values*

June, July, August and September are rainy and hence cloudy months in Ethiopia. As mentioned earlier, ArcGIS solar radiation tool do not consider the effects of clouds in the solar radiation calculation. Therefore, as figure 8 shows in summer the global solar radiation values calculated using ArcGIS solar radiation analysis tool was higher than solar radiation values recorded in the observational data.

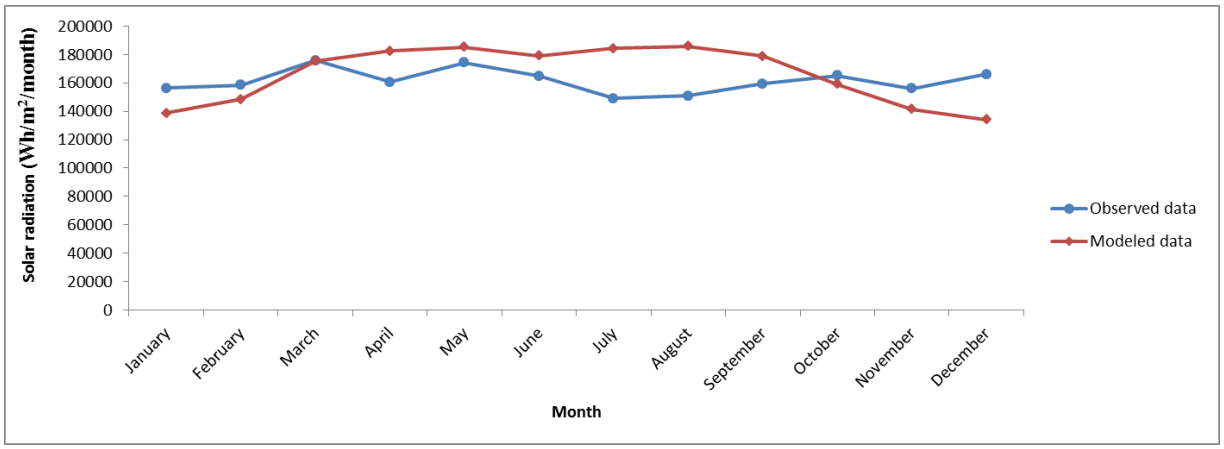

Figure 8: *Comparison between observed and modeled solar radiation value*

4.3 GIS-based Multi-Criteria Analysis

Solar radiation potential, slope, distance to road, distance to power transmission grid, population density, aspect, land cover and distance to water source were the selected criteria for suitability analysis for large scale PV solar farms in Ethiopia. As mentioned earlier, in order to create a suitability map that identifies potential sites, the input datasets needed to be changed into a raster with a common resolution. Therefore, these criteria datasets were converted into raster with 30 m resolution and reclassified from 1 to 5. 1, 2, 3, 4 and 5 indicates non-suitable, not suitable, marginally suitable, moderately suitable and highly suitable, respectively (table 6). Based on related literature and previous studies the selected criteria were defined as follows (Charabi & Gastli, 2011; Datta & Karakoti, 2010; Gastli & Charabi, 2010a; Janke, 2010; Li, 2013; Turney & Fthenakis, 2011; Uyan, 2013).

Table 5: *Suitability level per criteria for large-scale PV solar farms site selection*

Criteria	Measurement unit	Suitability level					Weight (%)
		5 Highly suitable	4 Moderately suitable	3 Marginally suitable	2 Not suitable	1 Non suitable	
Solar radiation	**MWh/m^2/year**	2.2 - 2.7	2.0 - 2.2	1.9 - 2.0	1.7 - 1.9	0.2 - 1.7	25.13
Slope	**%**	≤ 5	5 - 10	10 - 15	15 - 50	> 50	10.50
Population density	**Persons/km^2**	≤ 10	10 - 30	30 - 100	101 - 300	> 300	19.28
Land cover	**LCCS**	151 200 201 202	120 140 150	14 20 30 141	110 130 162 180	40 41 60 190 210	23.17
Aspect	**Direction**	South South East South West	East West	North East North West	North	Water surfaces	11.44
Distance to road	**km**	≤ 5	5 - 25	25 - 50	50 - 100	> 100	3.77
Distance to power transmission line	**km**	≤ 10	10 - 50	50 - 100	100 - 250	> 250	5.04
Distance to water	**km**	≤ 5	5 - 15	15 - 50	50 - 100	> 100	1.68

As shown in table 6, the annual solar radiation map of Ethiopia obtained from DEM was categorized into five classes and assigned discrete integer value for each class. Calculated mean solar radiation of the study area was 1.9 MWh/m^2/year. As a result, areas that receive greater than or equal to 2 MWh/m^2/year were considered as suitable site for large scale PV solar farms. Solar radiation was the most important criterion for large scale PV solar farms. Population density was the second most important criterion and calculated as number of persons per km^2. Since solar farms should avoid densely populated regions, sparsely populated areas with less than 30 persons per km^2 were taken as suitable sites for solar panel installations. The third important factor was existing land cover. According to land cover classification of FAO [11], twenty land cover types were identified in the study area and categorized into five classes. Bare areas, grassland, savannas and shrub lands were categorized as ideal land cover for large scale PV solar farms which is about one fourth of the total area. While populated, reserved and sensitive land covers such as forest, urban areas, water bodies and flooded areas were categorized as permanently unsuitable land cover. Large scale PV solar farms also require flat or gentle slope surfaces facing south and hence areas with less than 10 percent slope were considered as suitable. Moreover, distance to the existing infrastructure and water sources were also taken into account. These factors are important to minimize economic costs and increase the panel efficiency. Based on Euclidean distance, five classes were created and areas closer to existing road networks, power transmission lines and water sources considered as suitable for large-scale solar panel installations. To avoid dust and flood risk, areas within 1 km buffer zone of road and river networks were excluded from the final analysis. The results of the reclassification process of the eight input datasets are shown in the following figures.

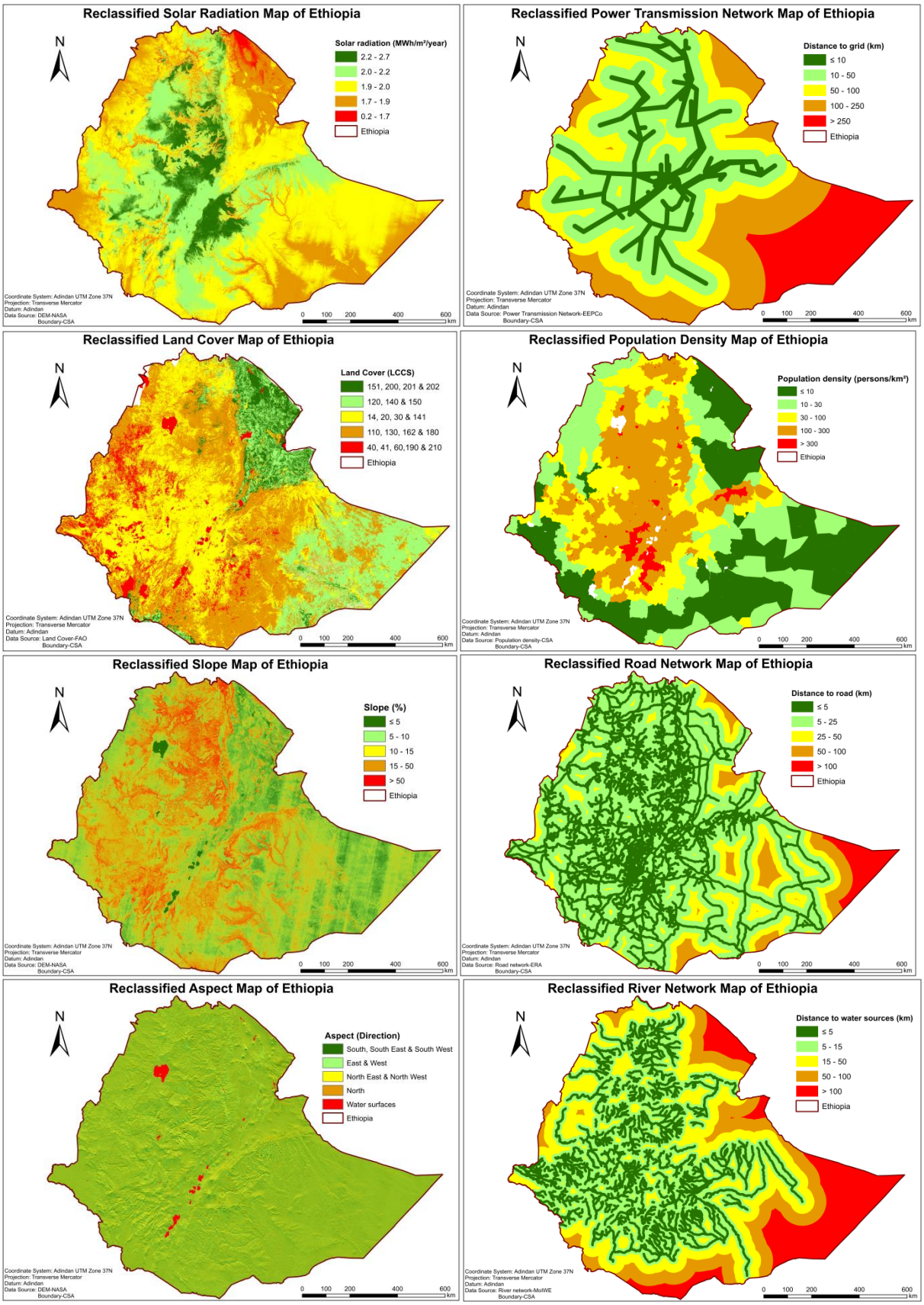

Figure 9: *Reclassified criteria datasets used in GIS-based multi-criteria analysis*

Using AHP a pairwise comparison matrix was created and criteria weights were calculated for each factor by comparing two factors at a time using a scale with values from 9 to 1/9 developed by (Saaty, 1988). The reclassified input datasets were assigned a weight value (table 4) to express the importance of each criterion to the other criteria for large-scale PV solar farms. In order to select suitable sites for large-scale PV installations all the reclassified input datasets were overlaid using the Weighted Overlay tool in ArcGIS. The result was a raster layer that indicates suitability score for solar farms between 0 and 1 as shown in figure 10. Pixel values close to 0 indicate permanently unsuitable areas and contrary pixel values near to 1 represents highly suitable site for large-scale solar panel installations.

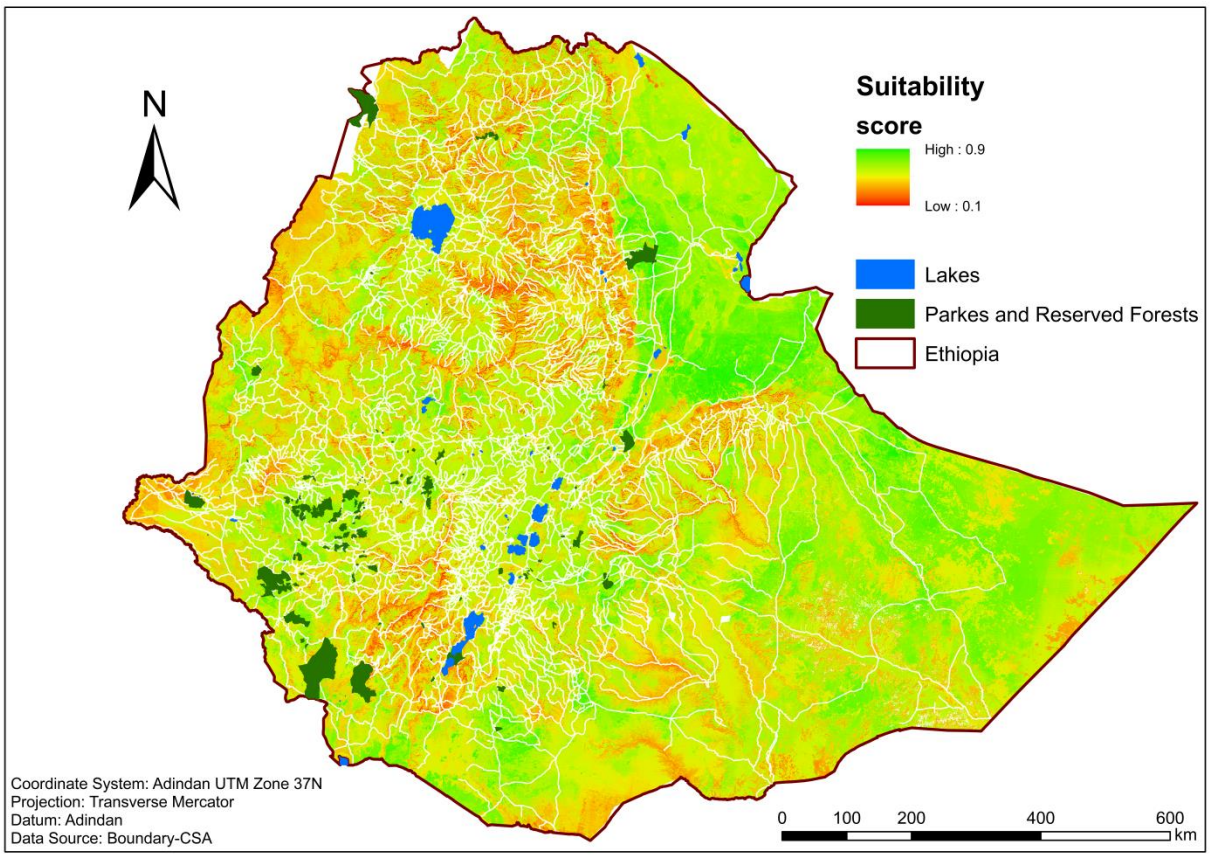

Figure 10: *Suitability map for large-scale PV solar farms in Ethiopia*

Therefore, for this study, pixels having suitability score of 0.75 or above were chosen as suitable and converted to polygons. Small polygons with areas less than 2.5 km^2 were filtered out and 195 large but compact shaped polygons with highest suitability score were mapped as potential sites for large scale PV solar farms in Ethiopia as shown in figure 11.

According to GIS-based MCA, the eastern part of the country is relatively suitable for large-scale solar panel installations. It has 1.9 MWh/m^2/year of solar radiation on average with ideal

land cover for large-scale solar farms. Moreover, it is the least densely populated region which also is a very important criterion.

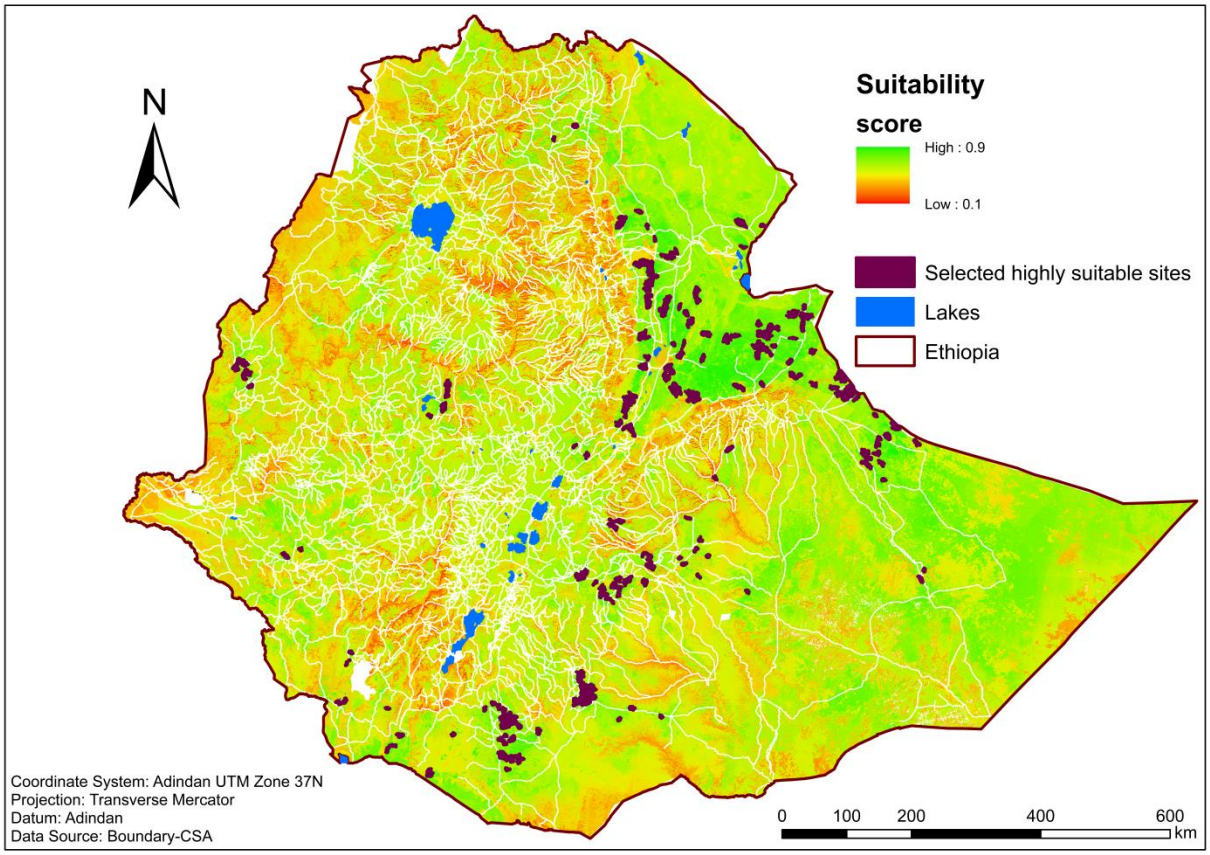

Figure 11: *Selected highly suitable sites for large-scale PV solar farms in Ethiopia*

4.4 Electricity Generation Potential

One aim of this study was to calculate average electricity generation potential of Ethiopia from PV systems. To estimate the annual electricity generation potential of the country from PV solar panels the following equation, which was previously employed by (Gastli & Charabi, 2010a) was used. The equation calculates the yearly potential based on mean solar radiation, total suitable area, and efficiency of PV system.

$$EGP = SR \times CA \times AF \times \eta$$

where:

EGP Electric power generation potential per year (GWh/year)

SR Annual solar radiation received per unit horizontal area (GWh/km^2/year)

CA Calculated total area of suitable land (km^2)

AF The area factor, indicates what fraction of the calculated areas can be covered by solar panels

η PV system efficiency

The estimated mean annual solar radiation for the suitable site was 1.9 TWh/km^2. The total suitable area for PV solar panel installation calculated using GIS-based MCA was close to 6,000 km^2 which accounts to 0.5 percent of the total area of Ethiopia. The electricity generation potential was computed by taking PV efficiency of five different solar cell materials. I have obtained the efficiency (η) values from the National Renewable Energy Laboratory of USA (Gaur & Tiwari, 2013; Green, Emery, Hishikawa, Warta, & Dunlop, 2012) [10]. The calculations also assume that at least 50 percent of the total area can be covered by solar panels. Annual potential of electricity generation from suitable sites for large scale PV solar farms using different types of Solar Cell materials computed as follows.

Table 6: *Estimated Electricity Generation Potential of Ethiopia*

Solar Cell materials	Efficiency (%)	Electricity Generation Potential	
		(GWh/year)	(GW)
Mono Crystalline Silicon (Mono C-Si)	25	1,423,752	162.5
Poly Crystalline Silicon (Poly C-Si)	20.4	1,161,782	132.6
Amorphous Silicon (a-Si)	10.1	575,196	65.7
Cadmium Telluride (CdTe)	18.3	1,042,187	119
Copper Indium Gallium Diselenide (CIGS)	20.3	1,156,087	132

As it clearly shown in table 7 selected highly suitable sites could, if exploited properly, generate more than 500 TWh electricity per annum using the lowest PV efficiency. According to EEPCo currently Ethiopia is producing only 7.5 TWh electricity, mainly from hydropower [14]. Therefore, it can be conclude that Ethiopia has very high potential to generate electricity from PV solar farms to meet the local and neighboring countries demand.

5 Discussions

In this section constraint regarding the DEM and other datasets used in this study to calculate solar radiations as well as to identify suitable sites for large-scale PV installations are discussed. Moreover, the sensitivity analysis, which was carried out by altering the weight values of each input criteria and comparisons of the results are presented as follows.

5.1 Data and factors

Monthly and annual global solar radiation of Ethiopia was calculated using Area solar radiation tool of the ArcGIS based on a Digital Elevation Model (DEM). To this end, 175 1° by 1° DEM tiles at 30 meter resolution cover the whole Ethiopia were downloaded from NASA. It is the most recent and highest resolution DEM with global coverage (Aster, 2010; Tachikawa, Hato, Kaku, & Iwasaki, 2011). Area Solar Radiation tool considers atmospheric effects, site latitude and elevation, slope, aspect, daily and seasonal shifts of the sun angle, the effects of shadows cast by the surrounding topography into calculation. These characteristics can be modelled from the DEM. Therefore, the DEM is the primary input for solar radiation calculation. The quality of calculated solar radiation output is dependent on DEM resolution as well as parameters such as time interval and sky size resolution. Higher resolution DEM with smaller time interval and bigger sky size results more accurate output but also increases considerable calculation time. Therefore, to achieve reasonable result at a short processing time the solar radiation map was calculated at 1,000 sky size with 0.5 hour interval.

GIS-based MCA was applied to select ideal locations for large-scale solar farms in Ethiopia. In this study large-scale refers to sites for ground-mounted PV installations with a minimum area of 2.5 km^2 on which 100 MW electricity can be generated from solar energy. In addition to solar radiation potential, various topographic, economic and environmental factors were taken into account in the site selection process. The most relevant factors for finding suitable sites for large-scale PV installations like solar radiation potential, land cover, land surface steepness, slope direction, distance to road network, and distance to existing power transmission lines, population density and distance from water features were considered. Some of these data were initially collected by concerned government organizations in 2007 or before. For instance, land cover and population density map of the study area represents data for the year 2005 and 2007, respectively. Since these data potentially are out of date, current data about population density, land cover are important to improve the results of this study.

5.2 Sensitivity analysis

To verify the results of the study, sensitivity analysis was carried out by altering the weight values of each input criteria under nine scenarios as shown in table 8. The weight value for each criterion was calculated using pair-wise comparison matrix of AHP with a consistency ratio of less than 10 percent.

Table 7: *Weight value (%) for each input criteria under nine scenarios*

	Scenario								
Criteria	**A**	**B**	**C**	**D**	**E**	**F**	**G**	**H**	**I**
Solar radiation	25.13	31.06	22.34	22.06	24.75	22.35	23.54	24.55	25.47
Land cover	23.17	20.31	28.38	19.86	21.51	21.39	21.78	22.28	23.41
Distance to power grid	5.04	4.99	4.97	5.16	4.95	8.84	4.05	4.91	5.10
Aspect	11.44	10.30	11.16	10.70	15.66	12.30	11.60	10.29	9.65
Slope	10.50	9.70	9.84	9.72	9.29	11.41	10.70	14.35	8.72
Distance to road	3.77	3.64	3.68	3.62	3.28	3.53	8.66	3.28	3.47
Distance to water source	1.68	1.69	1.66	1.64	1.66	1.59	1.55	1.64	4.54
Population density	19.28	18.31	17.96	27.23	18.89	18.59	18.11	18.70	19.65
Weight sum (%)	100	100	100	100	100	100	100	100	100
Consistency Ratio (%)	**6.40**	**7.73**	**7.87**	**9.04**	**7.35**	**9.91**	**7.38**	**9.62**	**6.61**
Total suitable area (%)	**0.88**	**0.47**	**1.13**	**1.44**	**1.02**	**0.87**	**1.12**	**1.01**	**0.56**

The suitability maps under each scenario were created using Weighted Sum tool of the ArcGIS and are shown in the following figures.

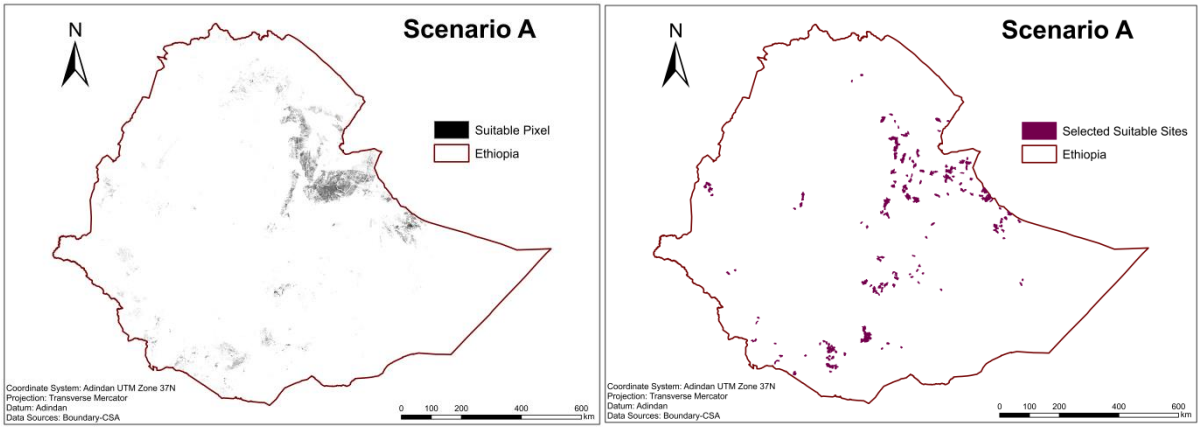

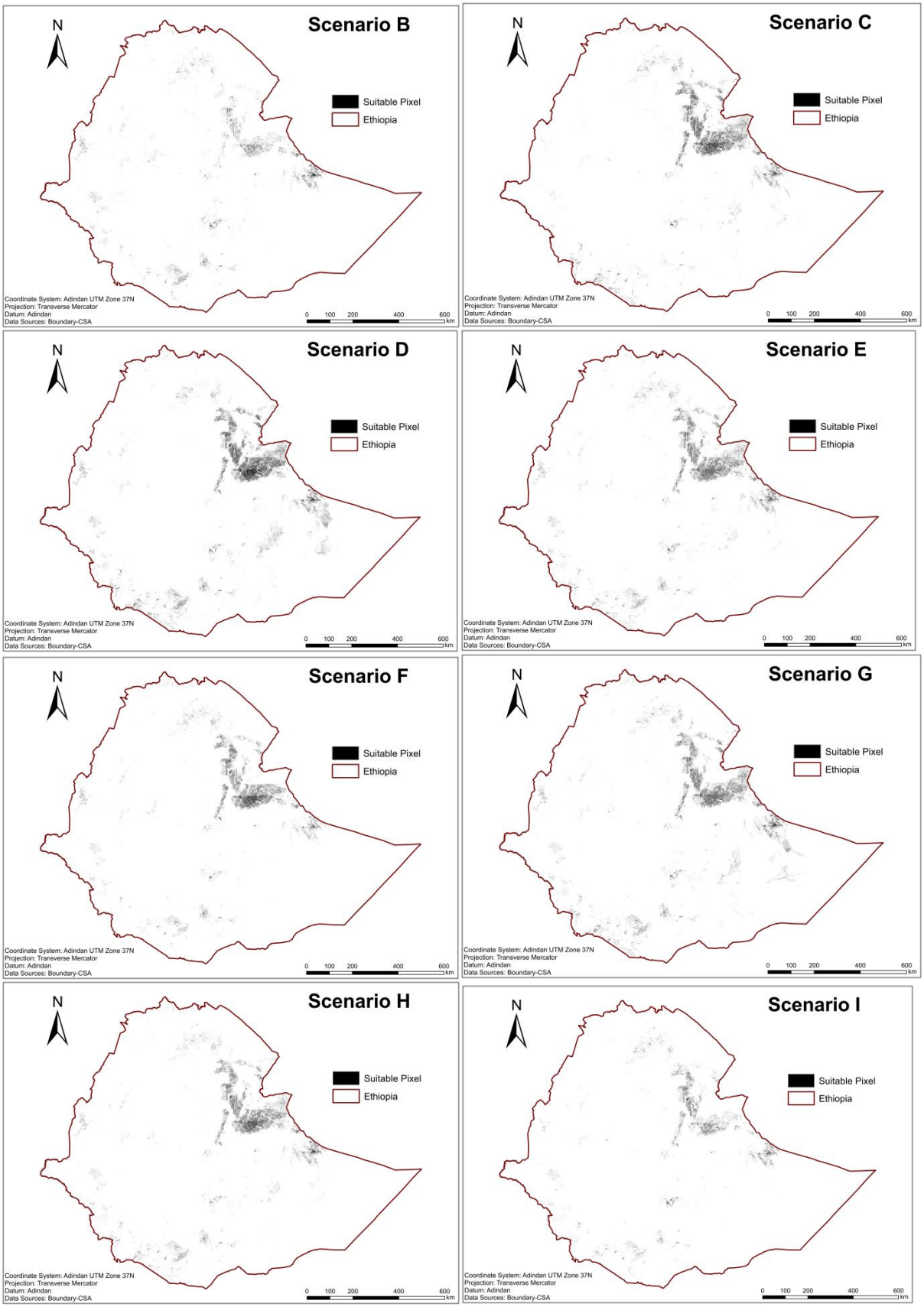

Figure 12: *Locations of suitable area (pixels) under nine scenarios*

In order to compare the effect of changes in weight value to the selection process, pixel with suitability score of greater than 0.75 were chosen as suitable pixel for large-scale PV installations. Scenario A is the base scenario where suitable sites for large-scale PV solar are selected in this study. According to the above figures, as the weight of solar radiation (scenario B) increases, total suitable size diminishes from 0.88 percent to 0.47 percent. In contrary, as the weight of land cover (scenario C) and population density (scenario D) increases, total suitable size grows by 128 percent and 164 percent, respectively. In scenario E a higher weight value were assigned to aspect than slope to test this effect. As a result, percentage of total suitable area was slightly increased from 0.88 to 1.02. Under scenario F and G the importance of distance to existing power grid and distance to road network were compared to each other. As distance to existing power grid increases from 5.04% to 8.84%, the sizes of suitable areas remain the same, whereas when distance to road network increases from 3.77 percent to 8.66 percent, percentage of suitable area grows with an increasing rate of 0.24 percent. Under scenario I, where distance to water sources increases from 1.68 percent to 4.84 percent, size of total suitable area decreases from 0.88 percent to 0.56 percent. As it is clearly shown from table 8 and figure 12, the sensitivity analysis of weight assignments under nine scenarios show the geographic locations of suitable sites with highest suitability scores remains the same with slight changes in size. In short, location of ideal sites under scenario A is robust and largely consistent regardless of moderate changes in the different parameters.

5.3 Comparisons

In total 195 sites located in different regions of Ethiopia were selected with aggregate electricity generation potential of 575 TWh/year from solar radiation. Geographic and absolute locations and characteristics of all the selected sites are presented under appendix D. Table 9 below shows the quantity and total areas of selected sites for large-scale PV installations as well as electricity generation potential per region. Based on the criteria presented in this study, the Somali, Oromia and Afar regions have the highest potential to generate electricity from ground-mounted PV solar panels.

Table 8: *Summary of selected sites per region*

Region	Number of Selected Sites	Total area (km^2)	Electricity Generation Potential (Twh/year)
Afar	30	1,228	118.5
Amhara	3	33	3.2
Baneshangul Gumuz	7	183	17.7
Gambella	1	24	2.3
Oromia	72	1,936	186.7
SNNP	7	102	9.8
Somali	73	2,429	234.4
Tigray	2	27	2.6
Ethiopia	195	5961.7	575.2

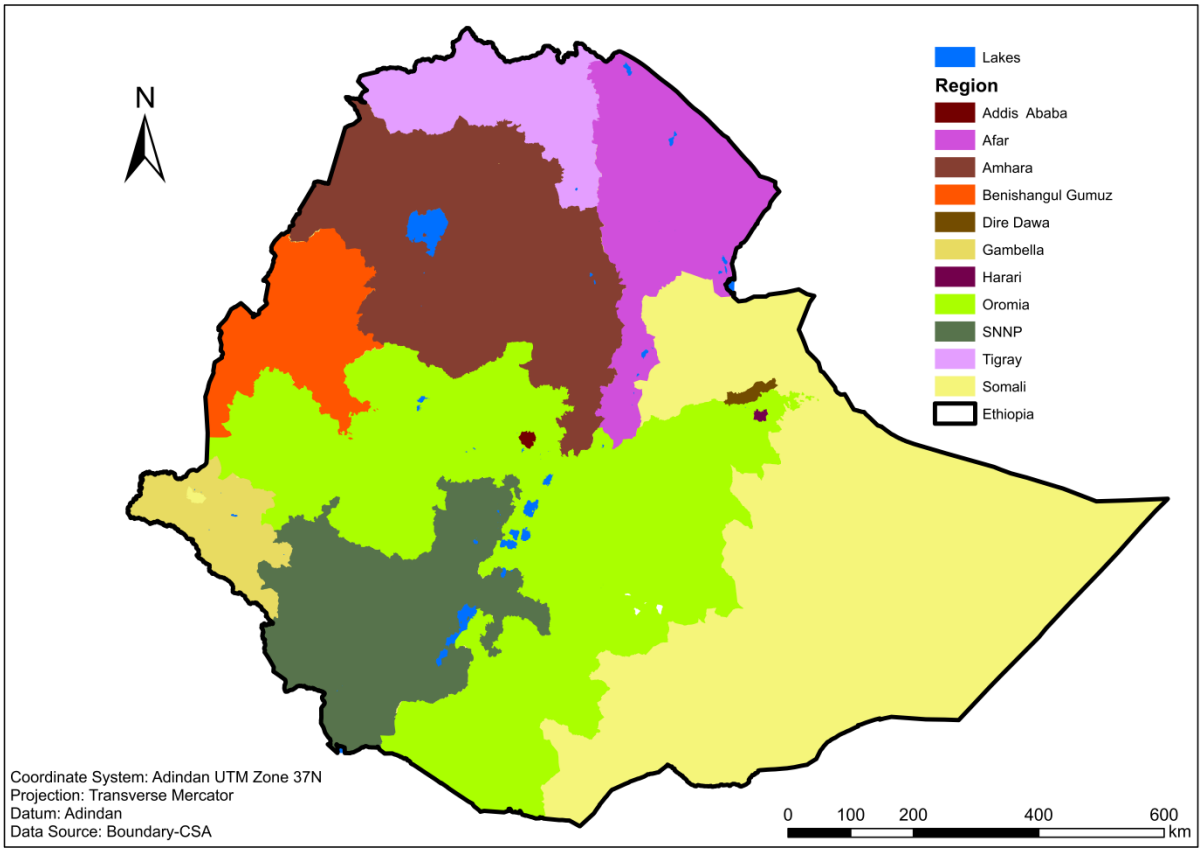

Figure 13: *Administrative regions of Ethiopia*

For comparison it is informative to compare this amount of power generation to some global numeric. According to the Wolfram Alpha computational knowledge engine, 575 GWh/year is equivalent to 65 GW, which is comparable to 1/35 of average global electric power production or 1/6 of electric power of all nuclear power plants on the globe [13]. This shows that Ethiopia has a very high potential to produce multiple times of the current annual

generation capacity. The total electric supply in 2012 was about 7,000 GWh [14]. Gastili and Charabi (2010) estimated yearly electricity generation potential of Oman from 1,500 km^2 highly suitable land area for PV installations as 360 GWh.

6 Limitations and future work

The accuracy of any GIS mapping and analysis output mainly dependent on the quality of input data and the tool. Improved data sources and incorporating additional criteria in the GIS-based MCA could improve the results of this study. Shortage of detailed, recent and digital spatial and attribute data in the study area was the main constraint of the study. Due to absence of higher resolution DEM or LiDAR imagery which cover the study area, I have used 30 m resolution DEM obtained from NASA to produce solar radiation potential map of Ethiopia. Since the quality depends on DEM resolution, estimation from higher resolution DEM such as 1 meter could produce highly reliable results. But this would also increase calculation time considerably and would be unfeasible without access to a super computer facility.

To test the accuracy of estimated solar radiation and to improve the tool by detecting sources of errors, latest ground measurement from several sample points representing different topography and climate recorded by an automatic solar radiation instrument such as Pyranometers are required. Absence of recent ground measurement from various meteorological stations forced me to use old and incomplete radiation values recorded using Actinographs from a few meteorological stations. Hence these data were not ideal to assess the reliability of the ArcGIS solar radiation tool.

Only solar radiation potential, population density, land cover, slope, aspect, distance to road network, distance to power transmission network and distance to water sources were taken into account in the GIS-based MCA for large scale PV solar farms in Ethiopia. Incorporating additional criteria such as future land use, wind speed, dust risk and, cultural heritage sites would improve the result obtained from the analysis and reduce risk of potential projects. Since there is no national standard and guidelines for solar PV installation in the country, I have defined the suitability levels of each criteria based on related studies conducted in other parts of the world and personal knowledge based criteria. Further field surveys and feasibility studies are necessary to verify the selected sites for large-scale PV installations.

Due to these limitations the suitability map provides a general overview of where large-scale PV farms could be located in Ethiopia. However, the study provides a good starting point for decision makers, governmental agencies and investors to evaluate Ethiopia as a promising candidate for large-scale PV solar power generation.

7 Conclusions

This study assesses solar energy potential of Ethiopia based on DEM using GIS. The obtained results show that there is a very high potential of solar power generation in extensive areas of Ethiopia throughout the year. The geographical location of Ethiopia, close to the equator and with large high altitude terrains, plays an important role. Using GIS-based multi-criteria analysis about 195 sites with 6000 km^2 area in total were selected as ideal locations for large scale PV solar farms in Ethiopia taking into account various topographic, economic, social and environmental factors. The factors used in this study have more of an effect at eliminating non-suitable areas for large-scale solar farms. If the selected sites could be exploited properly, they can generate more than 500 TWh electricity per annum using 10 percent PV efficiency, which is many times the current annual production.

References

Aster, G. (2010). Validation Team: METI/ERSDAC, NASA/LPDAAC, USGS/EROS, 2009. ASTER Global DEM Validation Summary Report.

Blumthaler, M., Ambach, W., & Ellinger, R. (1997). Increase in solar UV radiation with altitude. *Journal of photochemistry and Photobiology B: Biology, 39*(2), 130-134.

Bosch, J., Batlles, F., Zarzalejo, L., & López, G. (2010). Solar resources estimation combining digital terrain models and satellite images techniques. *Renewable Energy, 35*(12), 2853-2861.

Charabi, Y., & Gastli, A. (2010). GIS assessment of large CSP plant in Duqum, Oman. *Renewable and Sustainable Energy Reviews, 14*(2), 835-841.

Charabi, Y., & Gastli, A. (2011). PV site suitability analysis using GIS-based spatial fuzzy multi-criteria evaluation. *Renewable Energy, 36*(9), 2554-2561.

Datta, A., & Karakoti, I. (2010). *Solar Resource Assessment using GIS & Remote Sensing techniques.* Paper presented at the 11th ESRI India User Conference 2010.

Dickinson, W. C., & Cheremisinoff, P. N. (1980). *Solar energy technology handbook* (Vol. 2): Marcel Dekker New York.

Gastli, A., & Charabi, Y. (2010a). *Siting of large PV farms in Al-Batinah region of Oman.* Paper presented at the Energy Conference and Exhibition (EnergyCon), 2010 IEEE International.

Gastli, A., & Charabi, Y. (2010b). Solar electricity prospects in Oman using GIS-based solar radiation maps. *Renewable and Sustainable Energy Reviews, 14*(2), 790-797.

Gaur, A., & Tiwari, G. (2013). Performance of Photovoltaic Modules of Different Solar Cells. *Journal of Solar Energy, 2013*.

Green, M. A., Emery, K., Hishikawa, Y., Warta, W., & Dunlop, E. D. (2012). Solar cell efficiency tables (version 39). *Progress in photovoltaics: research and applications, 20*(1), 12-20.

Hardy, J. T. (2003). *Climate Change: Causes, effects, and solutions*: Wiley.

Janke, J. R. (2010). Multicriteria GIS modeling of wind and solar farms in Colorado. *Renewable Energy, 35*(10), 2228-2234.

Kaygusuz, K. (2001). Renewable energy: power for a sustainable future. *Energy, Exploration & Exploitation, 19*(6), 603-626.

Kumar, L. (2004). Reliability of GIS-based solar radiation models and their utilization in Agro-meteorlogical stations.

Kumar, L., Skidmore, A. K., & Knowles, E. (1997). Modelling topographic variation in solar radiation in a GIS environment. *International Journal of Geographical Information Science, 11*(5), 475-497.

Li, D. (2013). Using GIS and Remote Sensing Techniques for Solar Panel Installation Site Selection.

Malczewski, J. (1999). *GIS and multicriteria decision analysis*: John Wiley & Sons.

Martínez-Durbán, M., Zarzalejo, L., Bosch, J., Rosiek, S., Polo, J., & Batlles, F. (2009). Estimation of global daily irradiation in complex topography zones using digital elevation models and meteosat images: Comparison of the results. *Energy Conversion and Management, 50*(9), 2233-2238.

Mekonnen, S. A. (2007). *Solar Energy Assessment in Ethiopia: Modeling and Measurement.* Addis Ababa University.

Rich, P., Dubayah, R., Hetrick, W., & Saving, S. (1994). Using viewshed models to calculate intercepted solar radiation: applications in ecology. American Society for Photogrammetry and Remote Sensing Technical Papers.

Saaty, T. L. (1980). The analytic hierarchy process: planning, priority setting, resources allocation. *M cGraw-Hill*.

Saaty, T. L. (1988). *What is the analytic hierarchy process?* : Springer.

Šúri, M., Cebecauer, T., & Skoczek, A. (2011). *SolarGIS: solar data and online applications for PV planning and performance assessment.* Paper presented at the 26th European photovoltaics solar energy conference.

Šúri, M., Huld, T., Dunlop, E. D., & Hofierka, J. (2007). Solar resource modelling for energy applications *Digital Terrain Modelling* (pp. 259-273): Springer.

Šúri, M., Huld, T. A., Dunlop, E. D., & Ossenbrink, H. A. (2007). Potential of solar electricity generation in the European Union member states and candidate countries. *Solar energy, 81*(10), 1295-1305.

Tabik, S., Villegas, A., Zapata, E. L., & Romero, L. F. (2012). A fast GIS-tool to compute the maximum solar energy on very large terrains. *Procedia Computer Science*, *9*, 364-372.

Tachikawa, T., Hato, M., Kaku, M., & Iwasaki, A. (2011). *Characteristics of ASTER GDEM version 2.* Paper presented at the Geoscience and Remote Sensing Symposium (IGARSS), 2011 IEEE International.

Tadesse, M., & Belay, K. (2004). Factors influencing adoption of soil conservation measures in Southern Ethiopia: The case of Gununo area. *Journal of Agriculture and Rural Development in the Tropics and Subtropics (JARTS), 105*(1), 49-62.

Taha, R. A., & Daim, T. (2013). Multi-Criteria Applications in Renewable Energy Analysis, a Literature Review *Research and Technology Management in the Electricity Industry* (pp. 17-30): Springer.

Toman, M. T., & Jemelkova, B. (2003). Energy and economic development: an assessment of the state of knowledge. *The Energy Journal*(4), 93-112.

Tovar-Pescador, J., Pozo-Vázquez, D., Ruiz-Arias, J., Batlles, J., López, G., & Bosch, J. (2006). On the use of the digital elevation model to estimate the solar radiation in areas of complex topography. *Meteorological Applications, 13*(3), 279-287.

Turney, D., & Fthenakis, V. (2011). Environmental impacts from the installation and operation of large-scale solar power plants. *Renewable and Sustainable Energy Reviews, 15*(6), 3261-3270.

Uyan, M. (2013). GIS-based solar farms site selection using analytic hierarchy process (AHP) in Karapinar region, Konya/Turkey. *Renewable & Sustainable Energy Reviews, 28*, 11-17. doi: DOI 10.1016/j.rser.2013.07.042

Internet Sources

1. Environmental System Research Institute, ArcGIS resources ArcGIS help 10.2, *http://resources.arcgis.com/en/help/main/10.2/index.html#/Area_Solar_Radiation/009z000000t5000000/* (accessed in November, 2014)
2. Environmental System Research Institute, ArcGIS resources ArcGIS help 10.2, An overview of the Solar Radiation tools, *http://resources.arcgis.com/en/help/main/10.2/index.html#//009z000000t4000000* (accessed on October, 2014)
3. The Federal Democratic Republic of Ethiopia, Central Statistical Agency, *http://www.csa.gov.et* (accessed in March, 2013)
4. The Federal Democratic Republic of Ethiopia, Ethiopian Government Portal, *http://www.ethiopia.gov.et* (accessed in February, 2013)
5. The Federal Democratic Republic of Ethiopia, Ethiopian Meteorology Agency, *http://www.ethiomet.gov.et/* (accessed in March, 2014)
6. The US Central Intelligence Agency, The World Fact Book, *https://www.cia.gov/library/publications/the-world-factbook/geos/et.html* (accessed in October, 2013)
7. The US Environmental Protection Authority, *http://www.epa.gov/climatechange/science/future.html* (accessed in May, 2014)
8. The US National Aeronautics and Space Administration, Earth Observing System Data and Information System, *https://earthdata.nasa.gov/* (accessed in October, 2013)
9. The US National Aeronautics and Space Administration, Earth Observing System Data and Information System, *http://reverb.echo.nasa.gov/reverb/#utf8=%E2%9C%93&spatial_map=satellite&spatial_type=rectangle* (accessed in September, 2014)
10. The US National Renewable Energy Laboratory, Best Research Cell Efficiencies, *http://www.nrel.gov/ncpv/images/efficiency_chart.jpg* (accessed in April, 2014)
11. United Nations, Food and Agricultural Organizations, GeoNetwork, *http://www.fao.org/geonetwork/srv/en/main.home* (accessed in March 2014)

12. United Nations, Food and Agricultural Organizations, Global Land Cover Network, *http://www.glcn.org/activities/globcover_en.jsp* (accessed in March, 2014)

13. Wolfram Alpha computational knowledge engine, *https://www.wolframalpha.com/* (accessed in April, 2014)

14. The Federal Democratic Republic of Ethiopia, Ethiopian Electric Power Corporation, *http://www.eepco.gov.et/flyersandmagazines.php?rm=1* (accessed in December, 2013)

15. Environmental System Research Institute, Locating Sites for Photovoltaic Solar *http://www.esri.com/news/arcuser/1010/solarsiting.html* (accessed in February, 2013)

Appendix A: Observed Daily Global Solar Radiation of Meteorological Stations

daily Global solar radiation in cal/cm²/day

NATIONAL METEOROLOGICAL SERVICES AGENCY

Station: ADDIS ABABA(OBS) Wereda TEKLEHAIMANOT Awraja MENAGESHA Region SHOA

Alt. 2408 m Long. 38:45 Lat. 9:02 Element Daily solar radiation in CAL/CM²/DAY Year 1997

Brunna P.E.

Date	I	II	III	IV	V	VI	VII	VIII	IX	X	XI	XII	
1	408·2	436·4	478·6	337·8	549·0	436·4	281·5	281·5	x	x	478·6	x	
2	450·4	478·6	492·7	239·3	506·7	x	253·4	323·7	464·5	351·9	478·6	422·3	
3	366·0	x	x	239·3	563·0	422·3	267·4	337·8	366·0	534·9	x	436·4	
4	394·1	478·6	520·8	351·9	549·0	464·5	309·7	x	351·9	549·0	394·1	464·5	
5	422·3	492·7	520·8	323·7	x	394·1	337·8	309·7	295·6	478·6	478·6	422·3	
6	x	492·7	506·7	337·8	492·7	464·5	351·9	183·0	309·7	x	492·7	x	
7	394·1	464·5	492·7	x	549·0	450·4	x	323·7	478·6	422·3	492·7	x	
8	422·3	492·7	520·8	337·8	506·7	549·0	436·4	408·2	x	366·0	478·6	x	
9	394·1	478·6	450·4	351·9	534·9	x	168·9	309·7	464·5	464·5	366·0	408·2	
10	380·1	x	x	520·8	450·4	337·8	366·0	422·3	506·7	492·7	x	450·4	
	3631·6	3814·8	3923·5	3240·3	4701·4	3519·0	2773·0	2299·6	3237·5	3659·9	3859·9		
11	408·2	492·7	492·7	549·0	478·6	464·5	281·5	x	351·9	534·9	351·9	436·4	
12	436·4	464·5	450·4	492·7	x	464·5	309·7	323·7	478·6	492·7	337·8	464·5	
13	x	450·4	506·7	295·6	351·9	492·7	422·3	253·4	436·4	x	239·3	436·4	
14	267·4	478·6	x	x	549·0	366·0	x	309·7	351·9	464·5	295·6	492·7	
15	211·1	492·7	478·6	506·7	492·7	422·3	351·9	337·8	x	394·1	323·7	x	
16	168·9	506·7	492·7	422·3	577·1	x	380·1	323·7	520·8	309·7	366·0	478·6	
17	239·3	x	x	520·8	267·4	351·9	422·3	366·0	436·4	408·2	x	520·8	
18	323·7	464·5	492·7	366·0	394·1	337·8	394·1	x	520·8	351·9	267·4	478·6	
19	211·1	492·7	464·5	351·9	x	281·5	253·4	351·9	492·7	464·5	394·1	422·3	
20	x	478·6	408·2	x	422·3	380·1	351·9	394·1	506·7	x	436·4	450·4	
	2266·1	4321·4	3786·5	3505·2	3533·1	3561·3	3167·2	2660·3	4086·2	3420·5	3012·2		
21	140·8	464·5	534·9	x	450·4	478·6	x	366·0	380·1	351·9	295·6	464·5	
22	239·3	492·7	492·7	211·1	x	464·5	295·6	351·9	x	408·2	309·7	x	
23	309·7	492·7	337·8	295·6	492·7	x	380·1	323·9	478·6	x	337·8	464·5	
24	323·7	x	x	309·7	197·1	366·0	380·1	436·4	534·9	x	x	492·7	
25	323·7	464·5	x	366·0	422·3	281·5	366·0	x	x	450·4	351·9	x	
26	281·5	492·7	x	281·5	x	267·4	337·8	253·4	281·5	520·8	225·2	x	
27	x	478·6	x	267·4	450·4	422·3	225·2	323·7	478·6	x	295·6	366·0	
28	366·0	478·6	x	x	464·5	295·6	x	351·9	492·7	351·9	x	436·4	
29	422·3	—	x	506·7	436·4	351·9	309·7	450·4	x	351·9	478·6	x	
30	351·9	—	x	534·9	351·9	x	267·4	436·4	x	295·6	464·5	478·6	
31	436·4	—	x	—	351·9	—	309·7	436·4	—	464·5	—	520·8	
Sum	3195·3	3364·3	3366·4	2772·9	3617·6	2927·8	2871·6	3230·4	2646·4	3195·2	2958·9		
M. Sum	9093·8	11501·5	9135·4	9348·2	11852·1	10008·1	8811·8	9290·3	9980·1	10275·6	9431·0		
Mean	336·8	479·2	480·8	382·7	455·9	402·3	326·4	344·1	433·9	428·2	377·2	454·9	
Hig.													
Date													

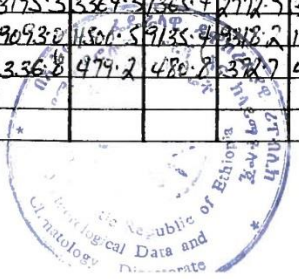

NATIONAL METEOROLOGICAL SERVICES AGENCY

Station: ARBAMINCH Wereda .... Awraja .... Region G. GOFFA

Alt. 1290 m Long. 37.38 Lat. 6.05 Element Daily Solar Radiation In CAL/CM2/DAY Year 1995

COMMERCIAL P. E. 43005//86

Date	I	II	III	IV	V	VI	VII	VIII	IX	X	XI	XII
1	475.2		118.8	451.4	x	451.4	415.8	308.9	332.6	439.6	451.4	439.6
2	427.7		x	534.6	499.0	499.0	x	166.3	332.6	356.4	451.4	451.4
3	392.0		163.3	487.1	510.8	x	451.4	154.4	451.4	403.9	392.0	475.2
4	439.6		x	534.6	510.8	522.7	392.0	320.8	415.8	522.7	368.3	475.2
5	403.9		x	190.1	427.7	510.8	415.8	213.8	225.7	463.3	487.1	499.0
6	451.4		x	380.2	451.4	522.7	415.8	403.9	x	392.0	487.1	487.1
7	439.6		x	427.7	403.9	534.6	190.1	451.4	x	368.3	451.4	427.7
8	451.4		x	x	522.7	522.7	332.6	261.4	427.7	451.4	451.4	487.1
9	451.4		x	427.7	510.8	522.7	249.5	332.6	427.7	x	499.0	451.4
10	463.3		x	522.7	499.0	487.1	356.4	522.7	522.7	x	499.0	463.3
	4350.5		382.1	3356.1	4556.1	4573.7	3209.4	3136.2	3136.2	[illegible]	[illegible]	4657.6
11	463.3		x	439.6	x	487.1	178.2	356.4	463.3	499.0	x	463.3
12	451.4		x	475.2	499.0	522.7	380.2	439.6	522.7	x	x	463.3
13	475.2		225.7	510.8	487.1	439.6	380.2	463.3	463.3	463.3	499.0	475.2
14	487.1		356.4	415.8	499.0	499.0	403.9	308.9	403.9	403.9	451.4	439.6
15	439.6		427.7	356.4	x	487.1	451.4	249.5	499.0	320.8	499.0	463.3
16	499.0		451.4	487.1	415.8	392.0	380.2	344.5	534.6	451.4	487.1	463.3
17	487.1		499.0	x	439.6	392.0	415.8	297.0	522.7	368.3	439.6	451.4
18	487.1		499.0	x	439.6	451.4	475.2	403.9	427.7	427.7	499.0	439.6
19	487.1		x	534.6	522.7	415.8	522.7	427.7	487.1	522.7	475.2	451.4
20	475.2		522.7	534.6	475.2	439.6	499.0	522.7	427.7	415.8	451.4	x
	4752.1		3981.9	3754.1	3792.0	4526.3	4026.2	3815.5	4752.0	3878.9	3801.7	4110.4
21	475.2		534.6	356.4	510.8	475.2	403.9	487.1	499.0	439.6	451.4	487.1
22	487.1		415.8	522.7	439.6	451.4	297.0	415.8	463.3	451.4	356.4	487.1
23	487.1		487.1	415.8	475.2	427.7	166.3	439.6	427.7	415.8	439.6	475.2
24	487.1		427.7	439.6	510.8	487.1	190.1	427.7	x	380.2	487.1	475.2
25	487.1		522.7	451.4	451.4	415.8	154.4	451.4	x	356.4	451.4	451.4
26	451.4		534.6	463.3	487.1	451.4	178.2	487.1	x	522.7	427.7	415.8
27	463.3	x	546.5	320.8	x	202.0	225.7	x	x	499.0	475.2	475.2
28	439.6	x	522.7	x	499.0	427.7	297.0	332.6	415.8	510.8	475.2	499.0
29	463.3		522.7	499.0	x	451.4	320.8	308.9	415.8	510.8	487.1	487.1
30			522.7	451.4	522.7	451.4	285.1	285.1	368.3	499.0	451.4	487.1
31			534.6	—	487.1	—	273.2	308.9	—	510.8	—	487.1
Sum	4241.2		5661.7	3920.4	4383.7	4241.9	2791.7					
M. Sum	13582.8		8871.7	11630.6	12497.8	13341.9	10057.7	[illegible]	[illegible]	12301.0	12842.3	13394.7
Mean	461.7		443.6	447.3	482.7	460.1	356.0	365	[illegible]	441.7	458.7	466.5
Hig.												
Date												
Low												
Date												

Copied by: Name Asnenafi Negash Sig. [signature] Checked by: Name .... Sig. ....
/tm.

NATIONAL METEOROLOGICAL SERVICES AGENCY

Station: BAHIR DAR (SYNOPTIC) Wereda BAHIR DAR Awraja BAHIR DAR Region GOJAM

Alt. 1770 m Long. 37.25 Lat. 11.36 Element Daily solar radiation in cal/cm²/day Year 1996

Branna P.E.

Date	I	II	III	IV	V	VI	VII	VIII	IX	X	XI	XII	
1	x	489.2	554.5	x	603.4	521.9	x	358.8	375.1	407.7	521.9	505.5	
2	472.9	505.5	538.2	538.2	570.8	570.8	570.8	391.4	x	538.2	472.9		
3	489.2	521.9	554.5	587.1	603.4	x	554.5	505.5	424.0	538.2	391.4		
4	521.9	538.2	x	538.2	570.8	472.9	456.6	489.2	424.0	472.9	x		
5	505.5	x	505.5	538.2	570.8	407.7	472.9	x	358.8	570.8	521.9		
6	505.5	489.2	554.5	570.8	x	391.4	456.6	342.5	309.9	521.9	472.9		
7	456.6	521.9	554.5	554.5	538.2	456.6	440.3	391.4	424.0	x	489.2		
8	x	505.5	570.8	x	456.6	407.7	x	358.8	375.1	521.9	472.9		
9	505.5	505.5	570.8	505.5	358.8	505.5	456.6	358.8	x	505.5	538.2		
10	456.6	538.2	570.8	554.5	260.9	x	456.6	293.5	570.8	554.5	505.5		
	3913.7	4615.1	4974.1	4387.0	4533.7	3734.5	3864.9	3485.9	3261.7	4631.6	4386.8		
11	472.9	538.2	x	554.5	407.7	521.9	538.2	407.7	489.2	521.9	x		
12	505.5	x	554.5	554.5	538.2	554.5	521.9	x	440.3	570.8	521.9		
13	489.2	538.2	554.5	x	x	538.2	309.9	391.4	375.1	554.5	472.9		
14	505.5	554.5	538.2	x	587.1	456.6	375.1	407.7	407.7	x	472.9		
15	x	521.9	570.8	x	570.8	456.6	x	375.1	440.3	570.8	342.5		
16	489.2	538.2	521.9	554.5	342.5	391.4	424.0	424.0	x	570.8	x		
17	505.5	521.9	554.5	538.2	391.4	x	456.6	505.5	538.2	505.5	x		
18	505.5	521.9	x	505.5	505.5	424.0	391.4	391.4	538.2	538.2	x		
19	456.6	x	554.5	538.2	472.9	603.4	538.2	x	489.2	554.5	391.4		
20	456.6	521.9	538.2	538.2	x	570.8	424.0	277.2	505.5	538.2	505.5		
	4386.5	4256.7	4387.1	3783.6	3816.1	4517.4	3879.3	3180.0	4223.7	4925.2	2707.1		
21	521.9	554.5	472.9	456.6	521.9	570.8	375.1	391.4	538.2	x	505.5		
22	x	554.5	424.0	x	587.1	505.5	x	424.0	489.2	521.9	489.2		
23	440.3	587.1	391.4	505.5	505.5	554.5	521.9	342.5	x	538.2	521.9		
24	505.5	554.5	489.2	587.1	538.2	x	472.9	424.0	505.5	554.5	505.5		
25	489.2	538.2	x	554.5	505.5	489.2	407.7	538.2	521.9	538.2	x		
26	489.2	x	489.2	554.5	440.3	603.4	521.9	x	505.5	538.2	472.9		
27	521.9	538.2	587.1	521.9	x	538.2	505.5	407.7	521.9	538.2	505.5		
28	538.2	538.2	554.5	554.5	407.7	505.5	570.8	440.3	472.9	x	489.2		
29	x	554.5	587.1	x	489.2	587.1	x	424.0	570.8	505.5	505.5		
30	505.5	—	521.9	603.4	440.3	554.5	375.1	440.3	x	538.2	505.5		
31	521.9	—	554.5	—	440.3	—	440.3	472.9	—	538.2	—		
Sum	4533.6	4449.7	5071.8	4338.0	4876.0	4908.7	4191.2	4305.3	4532.9	4811.1	4508.7		
M. Sum	12833.8	13291.5	14433.0	12508.6	13225.8	13360.6	12635.4	10975.2	9018.3	14367.8	11584.6		
Mean	493.6	531.7	465.6	543.9	489.8	506.2	462.9	406.5	360.7	538.1	483.1		
Hig.													
Date													
Low													
Date													

NATIONAL METEOROLOGICAL SERVICES AGENCY

Station: COMBOLCHA Wereda KALU Awraja KALU Region WELLO

Alt. 1903 M Long. 39°44 Lat. 11°07 Element Daily solar radiation in Cal/cm² /day Year 1985

Branna P.E.

Date	I	II	III	IV	V	VI	VII	VIII	IX	X	XI	XII	
1	X	386·1	339·8	401·5	X	293·4	401·5	278·0	370·7	308·9	355·2		
2	324·3	370·7	324·3	355·2	401·5	X	417·0	262·5	308·9	X	339·8		
3	308·9	370·7	X	X	432·4	355·2	X	216·2	339·8	X	386·1		
4	339·8	386·1	X	262·5	386·1	432·4	432·4	X	X	355·2	386·1	X	
5	X	386·1	X	308·9	417·0	X	432·4	X	X	262·5	370·7	355·2	
6	X	X	X	417·0	324·3	X	324·3	401·5	X	339·8	X	262·5	
7	308·9	339·8	X	216·2	386·1	432·4	X	X	X	293·4	308·9	370·7	
8	355·2	X	X	324·3	417·0	401·5	308·9	X	X	355·2	355·2	370·7	
9	X	X	X	386·1	478·8	X	370·7	231·7	X	X	386·1	370·7	
10	X	X	X	X	401·5	417·0	X	324·3	X	370·7	370·7	386·1	
	1637·1	2239·5	664·1	2671·7	3644·7	2331·9	2687·2	1714·2	2019·4	2285·7	3258·2		
11	X	X	X	386·1	401·5	447·9	401·5	339·8	X	417·0	355·2	X	
12	339·8	X	X	X	370·7	X	324·3	278·0	X	370·7	370·7	X	
13	370·7	X	X	401·5	447·9	X	339·8	216·2	X	370·7	X	X	
14	370·7	X	X	386·1	432·4	X	401·5	308·9	X	324·3	370·7	X	
15	355·2	X	X	370·7	X	X	386·1	308·9	X	308·9	370·7	X	
16	X	X	X	386·1	432·4	X	463·3	X	X	200·8	370·7	X	
17	370·7	X	X	X	X	386·1	X	X	X	308·9	401·5	X	
18	X	X	X	355·2	293·4	339·8	355·2	X	X	370·7	386·1	X	
19	X	X	X	386·1	324·3	X	X	247·1	262·5	386·1	370·7	293·4	
20	370·7	X	X	401·5	293·4	386·1	401·5	247·1	262·5	386·1	X	339·8	
	2177·8	–	–	3023·3	2996·0	1559·9	3073·2	1946·0	525·0	3444·2	2886·3	633·2	
21	370·7	X	X	447·9	X	386·1	324·3	X	X	401·5	355·2	355·2	
22	386·1	X	X	X	X	X	X	293·4	216·2	339·8	370·7	370·7	
23	X	339·8	X	432·4	447·9	417·0	139·0	355·2	247·1	X	278·0	370·7	
24	293·4	355·2	X	X	417·0	386·1	231·7	X	324·3	278·0	370·7	386·1	
25	293·4	X	432·4	X	432·4	355·2	262·5	308·9	X	370·7	355·2	X	
26	247·1	324·3	432·4	401·5	386·1	X	X	370·7	X	324·3	370·7	308·9	
27	X	X	X	324·3	401·5	X	X	339·8	370·7	339·8		X	
28	339·8	339·8	432·4	401·5	185·3	X	278·0	X	293·4	370·7		308·9	
29	370·7	–	417·0	432·4	X	417·0	200·8	247·1	216·2	370·7		355·2	
30	X	–	X	355·2	X	401·5	386·1	293·4	370·7	X		339·8	
31	X	–	401·5	–	447·9	–	X	355·2	–	355·2		216·2	
Sum	2361·2	1359·1	2115·7	2785·2	2718·1	2362·9	1822·4	2563·7	2038·6	3150·7		3011·7	
M. Sum	6116·1	3598·6	2779·8	8540·2	9358·8	6254·7	7582·8	6223·9	3583·0	8880·6			
Mean	339·8	359·9	397·1	371·3	390·0	390·9	344·7	296·4	298·6	341·6			
Hig.													
Date													
Low													
Date													

NATIONAL METEOROLOGICAL SERVICES AGENCY

Station: DERRE TABOR Wereda ____ Awraja ____ Region GONDAR

Alt. 2690 Long. 38·02 Lat. 11·53 Element Daily solar radiation in cal/cm²/day Year 1995

ARTISTIC PRINTERS 7139/79

Date	I	II	III	IV	V	VI	VII	VIII	IX	X	XI	XII
1	455·3	441·9	589·2	495·5	495·5	535·7	602·6	X	X	683·D	441·9	562·5
2		X	602·6	508·9	468·7	616·D	X	227·7	428·5	X	375·D	602·6
3		549·1	602·6	X	575·9	629·4	468·7	308·D	495·5	602·6	589·2	X
4		X	589·2	415·2	495·5	535·7	629·4	334·8	227·7	441·9	629·4	X
5		535·7	602·6	428·5	321·4	575·9	562·5	428·5	294·6	X	602·6	X
6		X	562·5	575·9	294·6	455·3	321·4	348·2	348·2	X	X	X
7		X	589·2	508·9	589·2	535·7	468·7	X	308·D	401·8	375·D	X
8		361·6	575·9	535·7	669·6	428·5	348·2	X	X	602·6	495·5	441·9
9		441·9	495·5	508·9	X	616·D	602·6	441·9	629·4	X	602·6	495·5
10		508·9	602·6	X	X	589·2	X	549·1	X	629·4	602·6	X
		2838·1	5811·3	3977·5	3910·4	5517·4	4024·1	3638·2	2731·9	3361·3	4713·2	2162·5
11		X	589·2	468·7	375·D	401·8	455·3	589·2	X	642·8	629·4	321·4
12		589·2	589·2	428·5	428·5	X	415·2	X	X	589·2	535·7	308·D
13		535·7	549·1	415·2	428·5	X	401·8	348·2	X	441·9	X	348·2
14		535·7	616·D	455·3	549·1	X	348·2	X	X	415·2	X	575·9
15		508·9	589·2	468·7	441·9	X	375·D	401·8	X	522·3	589·2	468·7
16		495·5	468·7	455·3	455·3	X	428·5	334·8	X	401·8	589·2	401·8
17		522·3	549·1	401·8	401·8	X	X	468·7	669·6	428·5	468·7	508·9
18		482·1	589·2	321·4	428·5	X	321·4	522·3	X	549·1	589·2	X
19		522·3	455·3	441·9	375·D	X	308·D	321·4	549·1	629·4	X	428·5
20		X	441·9	401·8	428·5	495·5	334·8	428·5	X	X	X	415·2
		4191·7	5436·9	4258·6	4312·1	8973	3388·2	3414·9	1218·7	4620·2	3401·4	3776·6
21		508·9	294·6	415·2	522·3	X	375·D	428·5	X	629·4	428·5	508·9
22		334·8	441·9	375·D	X	602·6	455·3	361·6	575·9	589·2	508·9	415·2
23		428·5	468·7	589·2	X	X	334·8	375·D	589·2	562·5	495·5	495·5
24		562·5	589·2	X	562·5	522·3	X	549·1	616·D	589·2	455·3	535·7
25		294·6	549·1	535·7	468·7	X	375·D	508·9	X	642·8	X	375·D
26		428·5	X	629·4	428·5	375·D	334·8	589·2	X	575·9	508·9	375·D
27		X	589·2	629·4	348·2	482·1	241·1	589·2	629·4	602·6	468·7	334·8
28		575·9	683·D	562·5	375·D	281·2	281·2	X	X	495·5	X	334·8
29		[illegible]	468·7	495·5	361·6	482·1	X	X	629·4	549·1	575·9	375·D
30	535·7	—	441·9	455·3	495·5	602·6	361·6	495·5	589·2	455·3	589·2	375·D
31	508·9	—	562·5	—	602·6	—	X	455·3	—	455·3	—	428·5
Sum		3133·7	5c 88·8	4687·2	4464·9	3347·9	2758·8	4352·3	3629·1	6146·8	4036·9	4553·4
M. Sum	1499·3	10164·5	16337·6	12823·3	12387·4	9762·6	10151·1	10465·4	7578·7	14128·3	12186·1	10422·9
Mean	500·D	484·D	544·6	478·6	458·8	513·8	406·D	435·6	505·3	583·4	628·1	434·7
Hig.												
Date												
Low												
Date												

Meteorological Climatology Directorate

NATIONAL METEOROLOGICAL SERVICES AGENCY

Station: DEDESSA Wereda .... Awraja .... Region WELLEGA

Alt. 1200 Long. 36.06 Lat. 9.23 Element Daily solar radiation in cal/cm²/day Year 1990

ARTISTIC PRINTERS 7139/79

Date	I	II	III	IV	V	VI	VII	VIII	IX	X	XI	XII
1	419.3	194.7	449.3	494.2	479.2	374.4	509.2	509.4	314.5	x	524.2	449.3
2	464.3	449.3	494.2	389.4	x	569.1	x	479.2	494.2	509.2	x	479.2
3	479.2	479.2	479.2	554.1	x	554.1	449.3	464.3	494.2	464.3	479.2	x
4	479.2	464.3	314.5	509.2	569.1	449.3	404.4	359.4	389.4	479.2	524.2	464.3
5	494.2	509.2	509.2	539.1	509.2	569.1	494.2	479.2	389.4	494.2	359.4	494.2
6	464.3	494.2	524.2	524.2	569.1	434.3	494.2	x	x	494.2	509.2	524.2
7	524.2	464.3	524.2	629.0	299.5	554.1	449.3	374.4	x	509.2	479.2	494.2
8	494.2	149.8	479.2	554.1	554.1	524.2	449.3	344.4	x	x	434.3	464.3
9	524.2	494.2	449.3	569.1	554.1	554.1	479.2	494.2	x	x	359.4	464.3
10	509.2	509.2	554.1	614.0	539.1	569.1	419.3	464.3	464.3	524.2	404.4	464.3
	4852.3	4203.4	4777.4	5376.4	4673.4	5151.8	4495.4	3368.2	2546.0	[illegible]	3073.5	4583.3
11	509.2	494.2	569.1	614.0	479.2	539.1	494.2	359.4	479.2	539.1	449.3	479.2
12	479.2	494.2	494.2	524.2	374.4	554.1	404.4	344.4	554.1	539.1	x	464.3
13	479.2	464.3	x	494.2	569.1	524.2	494.2	404.4	404.4	524.2	464.3	479.2
14	524.2	509.2	554.1	509.2	494.2	509.2	314.5	374.4	464.3	449.3	479.2	479.2
15	x	164.7	524.2	554.1	494.2	419.3	479.2	359.4	509.2	x	479.2	494.2
16	509.2	479.2	524.2	554.1	569.1	524.2	434.3	434.3	524.2	x	479.2	464.3
17	494.2	509.2	494.2	599.0	419.3	569.1	479.2	419.3	419.3	554.1	494.2	464.3
18	509.2	539.1	479.2	569.1	524.2	494.2	419.3	449.3	494.2	509.2	464.3	449.3
19	524.2	x	539.1	524.2	524.2	524.2	359.4	494.2	509.2	494.2	479.2	479.2
20	579.2	449.3	524.2	389.4	599.0	479.2	464.3	539.1	404.4	509.2	479.2	479.2
	4607.8	4103.4	4762.5	5331.5	5046.9	5136.8	4345.0	4178.2	4262.5	4113.4	4263.1	4732.4
21	494.2	494.2	479.2	524.2	554.1	494.2	344.4	374.4	524.2	524.2	494.2	464.3
22	464.3	x	464.3	599.0	569.1	524.2	x	434.3	479.2	539.1	509.2	479.2
23	494.2	479.2	479.3	464.3	569.1	554.1	x	389.4	404.4	554.1	509.2	494.2
24	479.2	179.7	614.0	554.1	524.2	554.1	494.2	419.3	524.2	554.1	494.2	
25	494.2	329.5	509.2	554.1	569.1	x	299.5	329.5	464.3	539.1	494.2	
26	464.3	x	539.1	479.2	569.1	509.2	374.4	524.2	509.2	509.2	494.2	
27	479.2	x	554.1	449.3	569.1	x	479.2	479.2	389.4	509.2	479.2	
28	509.2	419.3	479.2	479.2	464.3	509.2	629.0	464.3	554.1	x	494.2	
29	479.2	—	509.2	509.2	554.1	x	359.4	x	404.4	x	464.3	
30	464.3	—	569.1	569.1	449.3	x	x	494.2	509.2	524.2	404.4	
31	479.2	—	374.4	—	494.3	—	389.4	x	—	539.1	—	
Sum	5301.5	1901.9	5571.1	5181.7	5885.8	3145.0	3365.5	3908.8	4262.6	4792.3	4837.3	
M. Sum	14761.6	10213.7	15051.0	15889.6	15006.1	15433.6	11860.9	12055.8	12011.1	12385.2	13125.9	10468.4
Mean	492.1	425.6	508.7	529.7	517.5	516.7	439.3	430.6	464.3	[illegible]	476.7	425.8
Hig.												
Date												
Low												
Date												

Federal Democratic Republic of ... Meteorological Data and Climatology Directorate

NATIONAL METEOROLOGICAL SERVICES AGENCY

Station: DIRE DAWA Wereda SHEGOLLE Awraja DIRE DAWA ISA and GURGURA Region HARRARGE

Alt. 1260 m Long. 41·51 Lat. 9·36 Element Daily solar Radiation in Cal/cm²/day Year 1997

Branna P.E.

Date	I	II	III	IV	V	VI	VII	VIII	IX	X	XI	XII	
1	519·5	492·8	559·4	x	x	x	x	x	452·9	439·6	412·9	x	
2	506·2	572·8	532·8	x	572·8	452·9	x	x	x	399·6	452·9	506·2	
3	506·2	479·5	559·4	x	586·1	x	439·6	532·8	426·2	519·5	426·2	x	
4	492·8	532·8	546·1	x	572·8	x	492·8	519·5	452·9	319·7	399·6	x	
5	506·2	572·8	546·1	x	546·1	466·2	546·1	559·4	439·6	466·2	506·2	466·2	
6	506·2	559·4	546·1	x	492·8	439·6	519·5	559·4	346·3	439·6	426·2	506·2	
7	492·8	546·1	x	439·6	x	506·2	x	426·2	532·8	333·0	492·8	492·8	
8	506·2	559·4	466·2	x	x	x	492·8	572·8	x	333·0	506·2	506·2	
9	519·5	559·4	532·8	x	466·2	x	373·0	x	479·5	x	492·8	466·2	
10	519·5	x	479·5	x	452·9	492·8	519·5	x	519·5	x	559·4	506·2	
	5015·1	4825·6	4768·4	439·6	3689·7	2357·7	3383·5	3170·1	3649·7	3250·2			
11	532·8	559·4	506·2	x	x	x	559·4	x	452·9	532·8	519·5	466·2	
12	519·5	612·7	426·2	x	492·8	559·4	492·8	439·6	506·2	532·8	479·5	519·5	
13	506·2	572·8	559·4	x	466·2	x	559·4	x	466·2	599·4	412·9	519·5	
14	532·8	x	586·1	x	599·4	492·8	546·1	x	492·8	466·2	293·0	546·1	
15	519·5	559·4	532·8	x	x	492·8	546·1	x	x	466·2	466·2	506·2	
16	466·2	586·1	x	x	x	546·1	572·8	x	x	359·6	439·6	492·8	
17	492·8	559·4	x	506·2	x	466·2	479·5	x	466·2	239·8	412·9	519·5	
18	479·5	586·1	x	519·5	559·4	452·9	519·5	599·4	452·9	333·0	386·3	506·2	
19	519·5	586·1	x	452·9	x	x	546·1	x	452·9	386·3	386·3	479·5	
20	506·2	559·4	519·5	519·5	466·2	x	546·1	x	439·6	333·0	479·5	506·2	
	5125·0	5181·4	3130·2	1998·1	2584·0	3016·2	5367·8	1033·0	3729·7	4249·1			
21	479·5	572·8	559·4	359·6	586·1	506·2	572·8	x	452·9	213·1	319·7	492·8	
22	306·4	572·8	x	559·4	x	x	546·1	x	532·8	306·4	346·3	506·2	
23	173·2	586·1	506·2	559·4	x	546·1	572·8	x	532·8	x	506·2	399·6	
24	306·4	572·8	x	506·2	x	572·8	572·8	x	586·1	x	399·6	492·8	
25	333·0	559·4	x	519·5	399·6	546·1	506·2	x	412·9	x	293·0	479·5	
26	306·4	586·1	x	506·2	386·3	x	x	559·4	492·8	x	278·7	439·6	
27	492·8	559·4	x	599·4	546·1	559·4	x	519·5	532·8	x	359·6	399·6	
28	x	532·8	559·4	x	x	519·5	559·4	x	426·2	x	452·9	452·9	
29	452·9	—	452·9	559·4	466·2	506·2	559·4	x	492·8	x	492·8	506·2	
30	506·2	—	386·3	x	572·8	x	572·8	519·5	426·2	386·3	479·5	519·5	
31	519·5	—	x	—	x	—	x	546·1	—	x	—	532·8	
Sum	3876·3	4542·2	2464·2	4169·1	2957·1	3756·3	4462·3	2944·5	4888·3	905·8			
M. Sum	14026·4	14598·6	11362·8	6606·8	9230·8	9124·2	13213·4	6353·6	12267·7	8405·1			
Mean	467·5	561·5	518·1	508·2	512·8	506·9	528·5	529·5	471·8	460·2			
Hig.													
Date													

NATIONAL METEOROLOGICAL SERVICES AGENCY

Station: METEHARA Wereda FENTALE Awraja YERER È KEREYU Region SHOA

Alt. 930 Long. 39·54 Lat. 8·52 Element Daily Solar Radiation In CAL/CM2/DAY Year 1996

COMMERCIAL P. E. 43005/86

Date	I	II	III	IV	V	VI	VII	VIII	IX	X	XI	XII
1	X	491·5	419·6	X	503·5	479·5	X	491·5	X	455·5	455·5	479·5
2	419·6	467·5	515·5	503·5	527·5	467·5	431·6	491·5	X	455·5	455·5	X
3	419·6	467·5	503·5	515·5	503·5	X	467·5	491·5	335·7	455·5	455·5	467·5
4	X	479·5	X	515·5	491·5	431·6	455·5	443·6	491·5	503·5	X	467·5
5	X	X	503·5	515·5	X	335·7	467·5	347·7	491·5	479·5	467·5	443·6
6	395·6	467·5	503·5	467·5	X	239·8	479·5	467·5	395·6	443·6	467·5	479·5
7	335·7	491·5	467·5	395·6	503·5	311·7	251·7	443·6	383·6		455·5	443·6
8	X	479·5	467·5	X	395·6	443·6	X	467·5	443·6		491·5	455·5
9	503·5	479·5	479·5	515·5	407·6	479·5	419·6	419·6	X		467·5	X
10	479·5	479·5	479·5	503·5	383·6	X	X	443·6	407·6		467·5	455·5
	2553·5	4303·5	4339·6	3928·1	3716·3	3188·3	2972·9	4507·6	2947·1		4183·5	3652·2
11	443·6	491·5	X	503·5	455·5	467·5	299·7	299·7	467·5		X	455·5
12	X	X	479·5	491·5	503·5	419·6	419·6	X	455·5		455·5	419·6
13	X	491·5	491·5	491·5	X	419·6	X	467·5	455·5		443·6	443·6
14	X	491·5	467·5	503·5	503·5	443·6	395·6	479·5	479·5	X	443·6	455·5
15	X	479·5	491·5	X	407·6	471·6	X	419·6	419·6	491·5	431·6	455·5
16	395·6	467·5	419·6	491·5	503·5	275·7	395·6	383·6	X	479·5	443·6	X
17	X	419·6	467·5	503·5	419·6	X	431·6	467·5	491·5	431·6	179·8	431·6
18	X	455·5	X	479·5	419·6	383·6	335·7	479·5	455·5	407·6	X	443·6
19	443·6	X	443·6	467·5	371·6	479·5	383·6	X	467·5	419·6	335·7	443·6
20	X	467·5	X	275·7	X	467·5	419·6	467·5	443·6	479·5	455·5	419·6
	1288·8	3764·1	3260·7	4207·7	3584·4	3228·2	3081·0	3464·4	4235·7		3188·3	3968·1
21	479·5	491·5	455·5	467·5	383·6	479·5	431·6	395·6	431·6	X	455·5	443·6
22	X	467·5	383·6	X	467·5	467·5	X	491·5	443·6	479·5	467·5	431·6
23	431·6	479·5	X	515·5	515·5	467·5	407·6	431·6	X	491·5	X	X
24	491·5	467·5	X	539·5	431·6	X	215·8	203·8	419·6	479·5	407·6	419·6
25	455·5	467·5	X	287·7	467·5	467·5	239·8	289·7	455·5	491·5	X	407·6
26	443·6	X	X	479·5	383·6	491·5	443·6	X	419·6	491·5	X	407·6
27	419·6	467·5	X	419·6	X	455·5	443·6	467·5	455·5	479·5	467·5	443·6
28	455·5	455·5	X	467·5	503·5	479·5	443·6	503·5	491·5	X	479·5	419·6
29	X	455·5	X	X	503·5	467·5	X	455·5	455·5	479·5	455·5	431·6
30	491·5	—	X	X	419·6	467·5	395·6	407·6	X	479·5	467·5	X
31	479·5	—	X	—	407·6	—	491·5	X	—	491·5	—	431·6
Sum	4147·8	3752·0	3339·1	3176·8	4483·5	4243·5	3512·7	3656·3	3572·4	4363·5	3200·6	3836·4
M. Sum	7984·1	11819·6	8438·4	11316·6	11784·2	11260·6	9566·6	11628·3	11657·2		10573·0	11496·7
Mean	443·6	472·8	468·9	471·5	453·2	433·1	398·6	483·7	444·5		440·5	442·2
Hig.												
Date												
Low												
Date												

Copied by: Name ASHENAFI NEGASH Sig. ..... Checked by: Name ..... Sig. .....

/tm.

National Meteorological Data and Technology Directorate

NATIONAL METEOROLOGICAL SERVICES AGENCY

Station: NAZARETH Wereda ADAMA Awraja YERER & KEREYU Region SHEWA

Alt. 1622 m Long. 39:17 Lat. 8:33 Element Daily solar radiation in cal/cm²/day Year 1982

Branna P.E.

Date	I	II	III	IV	V	VI	VII	VIII	IX	X	XI	XII	
1			519·8	X	574·6	588·2	601·9	X	X	560·9	588·2	X	
2			588·2	X	560·9	X	547·2	X	684·0	588·2	560·9	533·5	
3		X	X	X	574·6	574·6	383·0	X	629·3	574·6	X	574·6	
4		X	574·6	X	601·9	533·5	629·3	X	X	601·9	560·9	519·8	
5		560·9	588·2	X	X	451·4	519·8	X	643·0	588·2	506·2	547·2	
6		601·9	588·2	X	615·6	492·5	492·5	506·2	588·2	X	547·2	560·9	
7		601·9	574·6	X	533·5	X	X	451·4	643·0	478·8	574·6	547·2	
8		615·6	560·9	383·0	670·3	601·9	506·2	601·9	X	506·2	574·6	X	
9		601·9	588·2	519·8	643·0	X	205·2	492·5	670·3	492·5	547·2	574·6	
10		X	X	465·1	643·0	588·2	615·6	588·2	629·3	547·2	X	519·8	
			4562·7	1367·9	5417·4	3833·3	4508·7	2646·2	4487·1	4935·5			
11		574·6	560·9	574·6	643·0	629·3	451·4	X	574·6	643·0	574·6	560·9	
12		574·6	601·9	547·2	X	615·6	615·6	643·0	656·6	601·9	451·4	519·8	
13		574·6	574·6	410·4	560·9	X	588·2	383·0	601·9	X	478·8	478·8	
14		588·2	588·2	X	656·6	629·3	X	643·0	670·3	560·9	465·1	574·6	
15		588·2	X	588·2	656·6	615·6	684·0	656·6	X	560·9	588·2	X	
16		588·2	560·9	601·9	643·0	X	643·0	X	643·0	492·5	533·5	583·5	
17		X	X	533·5	X	X	519·8	X	615·6	424·1	X	547·2	
18		588·2	547·2	574·6	X	629·3	X	X	684·0	437·8	506·2	533·5	
19		588·2	X	588·2	X	424·1	X	643·0	629·3	369·4	519·8	533·5	
20		588·2	X	396·7	X	643·0	X	601·9	643·0	X	560·9	533·5	
		5253·0	3433·7	4215·3	3160·1	4188·2	3562·0	3570·5	5718·3	4096·5			
21		574·6	588·2	X	X	615·6	X	643·0	629·3	369·4	506·2	519·8	
22		601·9	588·2	492·5	X	560·9	X	601·9	X	560·9	519·8	X	
23		601·9	492·5	328·3	X	X	X	656·6	670·3	465·1	560·9	519·8	
24		X	X	506·2	X	643·0	X	506·2	689·3	287·3	X	560·9	
25		601·9	424·1	506·2	X	574·6	X	X	643·0	560·9	478·8	519·8	
26		601·9	X	478·8	X	574·6	560·9	643·0	560·9	533·5	369·4	533·5	
27		X	396·7	383·0	615·6	643·0	643·0	601·9	588·2	X	492·5	506·2	
28		588·2	519·8	X	601·9	X	X	383·0	615·6	342·0	492·5	533·5	
29		—	533·5	574·6	574·6	X	629·3	670·3	X	478·8	560·9	X	
30		—	492·5	506·2	601·9	X	629·3	X	601·9	465·1	519·8	478·8	
31		—	X	—	533·5	—	383·0	X	—	583·5		560·9	
Sum		3570·4	9035·5	3795·8	2827·5	3611·7	2845·5	4765·9	4938·5				
M. Sum			12651·9	9959·0	11505·0	11628·2	10848·2	10916·6	15143·9				
Mean			547·8	498·0	605·5	581·4	542·4	574·6	631·0				
Hig.													
Date													
Low													
Date													

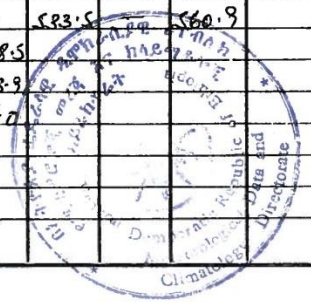

NATIONAL METEOROLOGICAL SERVICES AGENCY

Station: WELAYITA SODO Wereda ..... Awraja WELAYITA Region SIDAMO

Alt. 1800 M Long. 37°45 Lat. 6°51 Element Daily Solar Radiation In Cal/cm²/day Year 1992

Branna P.E.

Date	I	II	III	IV	V	VI	VII	VIII	IX	X	XI	XII	
1	411·5	466·3	397·8	452·6	480·1	493·8	288·0	342·9	X	411·5	452·6		
2	411·5	480·1	493·8	219·5	507·5	X	384·0	233·2	480·1	480·1	X		
3	425·2	X	X	315·5	521·2	480·1	329·2	397·8	411·5	411·5	425·2		
4	356·6	466·3	480·1	X	507·5	507·5	X	X	425·2	466·3	X		
5	246·9	480·1	480·1	384·0	X	466·3	466·3	356·6	480·1	452·6	438·9		
6	X	452·6	493·8	438·9	480·1	384·0	301·8	356·6	X	438·9	438·9		
7	329·2	466·3	480·1	X	397·8	521·2	X	342·9	480·1	438·9	466·3		
8	411·5	507·3	466·3	X	452·6	X	288·0	260·9	X	411·5	480·1		
9	342·9	493·8	480·1	452·6	425·2	452·6	315·5	X	411·5	493·8	397·8		
10	384·0	466·3	X	288·0	452·6	452·6	397·8	384·0	425·2	411·5	X		
	3319·3	4279·1	3772·1	2551·1	4224·6	3758·1	2770·6	2674·9	3113·7				
11	356·6	466·3	480·1	X	452·6	480·1	384·0	X	466·3	480·1	356·6		
12	411·5	480·1	466·3	493·8	X	411·5	342·9	438·9	356·6	384·9	397·8		
13	X	438·9	411·5	315·5	425·2	438·9	397·8	411·5	370·3	X	274·3		
14	384·0	466·3	480·1	X	466·3	274·3	X	480·1	425·2	480·1	246·9		
15	301·8	411·5	466·3	466·3	466·3	438·9	356·6	X	X	384·0	X		
16	342·9	438·9	438·9	493·8	521·2	X	342·9	X	452·6	384·0	288·0		
17	X	X	X	X	329·2	384·0	397·8	466·3	438·9	411·5	X		
18	370·3	480·1	480·1	466·3	493·8	342·9	493·8	X	384·0	301·8	452·6		
19	X	X	425·2	384·0	X	288·0	X	X	466·3	260·6	370·3		
20	329·2	493·8	452·6	411·5	493·8	301·8	178·3	397·8	X	X	425·2		
	2496·3	3675·9	4101·1	3031·2	3648·4	3360·4	2834·1	2194·6	3360·2				
21	329·2	493·8	493·8	X	480·1	329·2	X	315·5	466·3	397·8	356·6		
22	301·8	480·1	466·3	260·6	452·6	384·0	X	219·5	X	356·6	356·6		
23	315·5	507·5	480·1	356·6	507·5	370·3	X	466·3	329·2	301·8	411·5		
24	384·0	X	X	452·6	X	342·9	X	480·1	466·3	370·3	X		
25	342·9	X	370·3	342·9	507·5	452·6	X	X	370·3	466·3	370·3		
26	356·6	480·1	301·8	480·1	X	411·5	219·5	384·0	329·2	342·9	342·9		
27	X	493·8	384·0	301·8	493·8	466·3	466·3	370·3	288·0	X	411·5		
28	384·0	480·1	452·6	X	X	X	X	301·8	438·9	356·6	425·2		
29	480·1	—	438·9	493·8	342·9	425·2	301·8	438·9	X	356·6	452·6		
30	438·9	—	246·9	329·2	507·5	X	425·2	452·6	384·0	288·0	425·2		
31	356·6	—	X	—	507·5	—	315·5	X	—	425·2	—		
Sum	3689·6	7935·4	3634·7	3017·6	3799·4	3182·0	1728·3	3429·0					
M. Sum	9505·2	10890·4	11507·9	8599·9	11672·4	10300·5	7383·0	8298·5					
Mean	365·6	473·5	442·6	390·9	466·4	412·0	352·0						
Hig.													
Date													

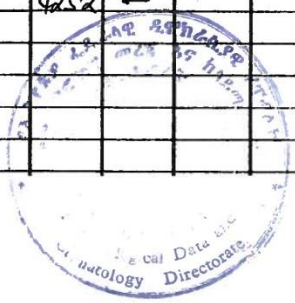

Appendix B: GIS Models for Solar Radiation Calculation

GIS Model to create 1° latitude zone by mosaic 1° by 1° DEM tile of a particular degree latitude

(Repeated to create 13 major zones and 11 minor DEM zones)

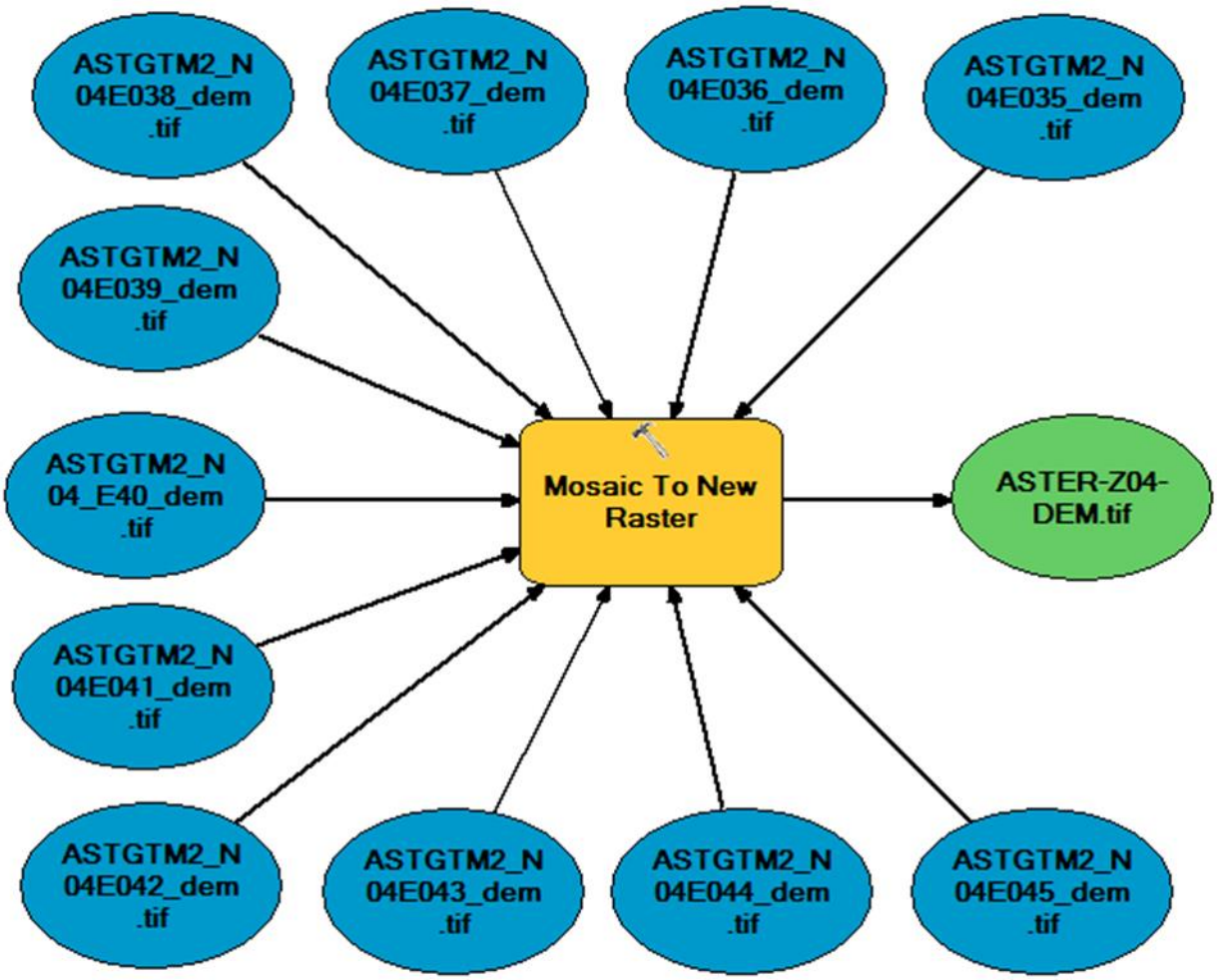

GIS Model to calculate solar radiation for a major zone using Area Solar Radiation Tool and appropriate parameters

(Repeated to calculate solar radiation for each major and minor zone)

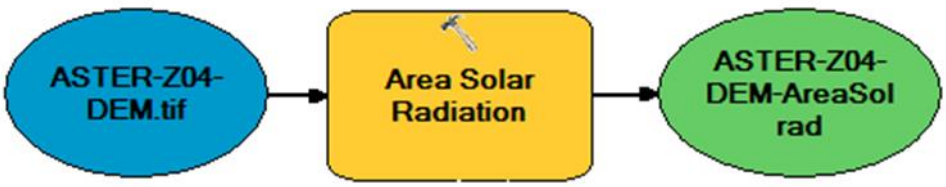

GIS Model to calculate Monthly Global Radiation of Ethiopia by mosaic all major and minor zones' solar radiation of a particular month

(Repeated to calculate Global Solar Radiation for each month in a Year)

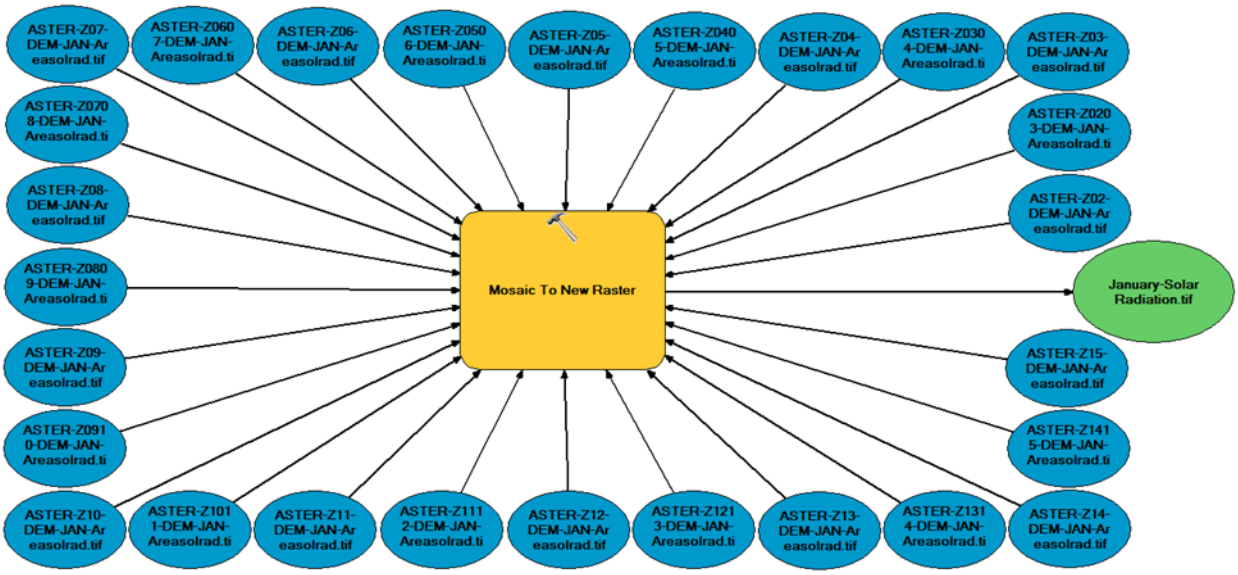

GIS Model to obtain Annual Global Solar Radiation of Ethiopia by Mosaic Monthly Global Radiation of Months in a Year

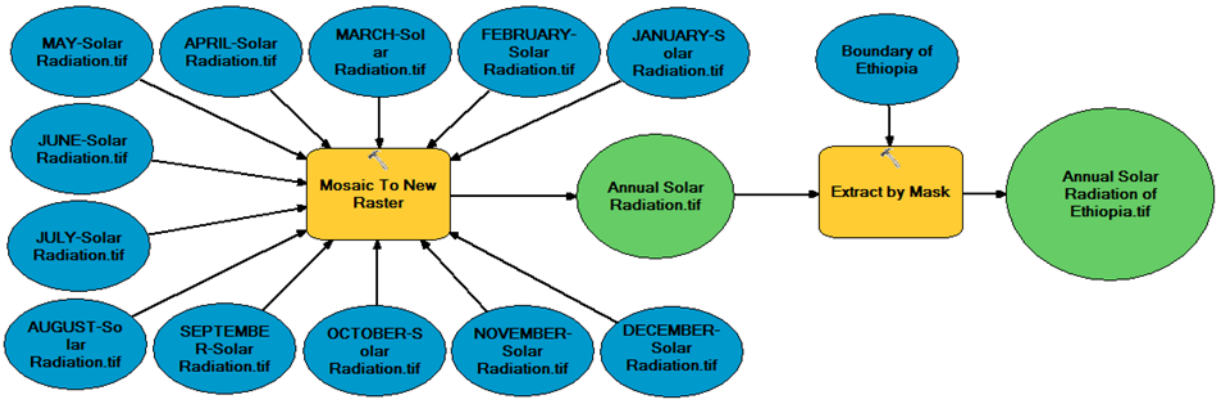

GIS Model to calculate Global Solar radiation of a Meteorological Station using Point Solar Radiation Tool and appropriate parameters

(Repeated to calculate Global Solar Radiation for each Sample Meteorological Station)

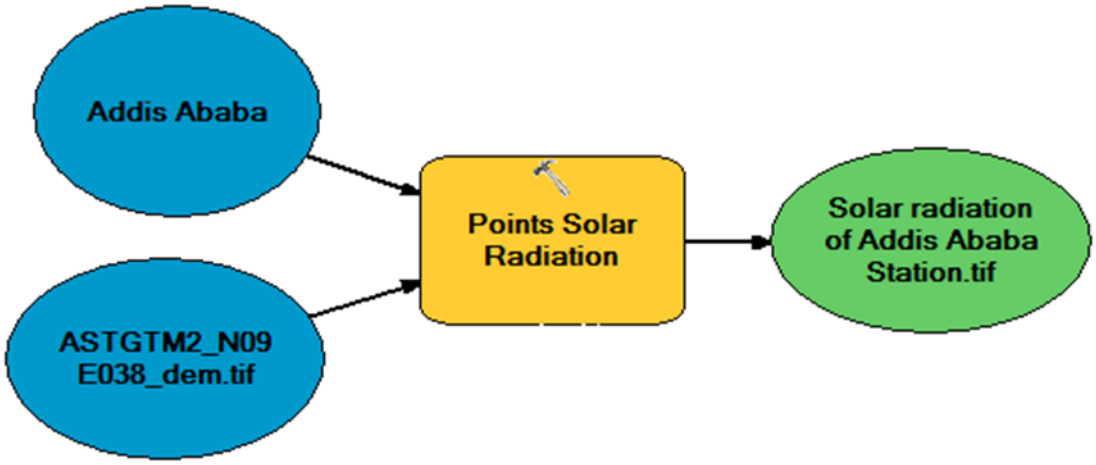

Appendix C: GIS Models for GIS-Based Multi-Criteria Site Selection for Large-Scale PV Installations in Ethiopia

GIS Model to Project and Reclassify Annual Solar Radiation Raster into Five Suitability Level

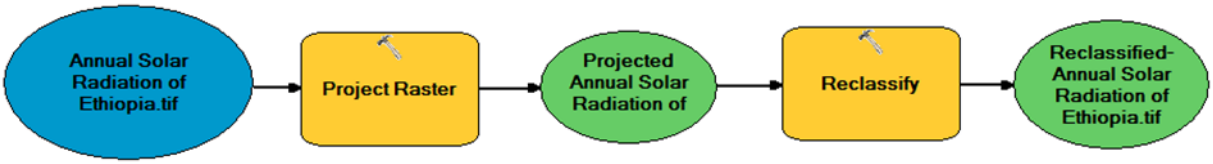

GIS Model to calculate Euclidean Distance around Road, River and Power Transmission Lines and to Project and Reclassify the output Raster into Five Suitability Level

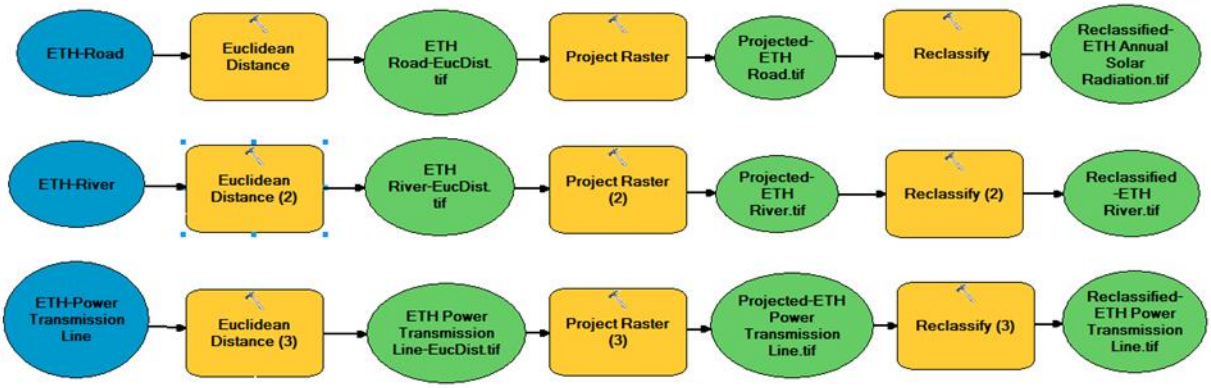

GIS Model to Derive Aspect and Slope from Mosaic ASTER DEM of Ethiopia and to Project and Reclassify the Aspect and Slope Raster into Five Suitability Level

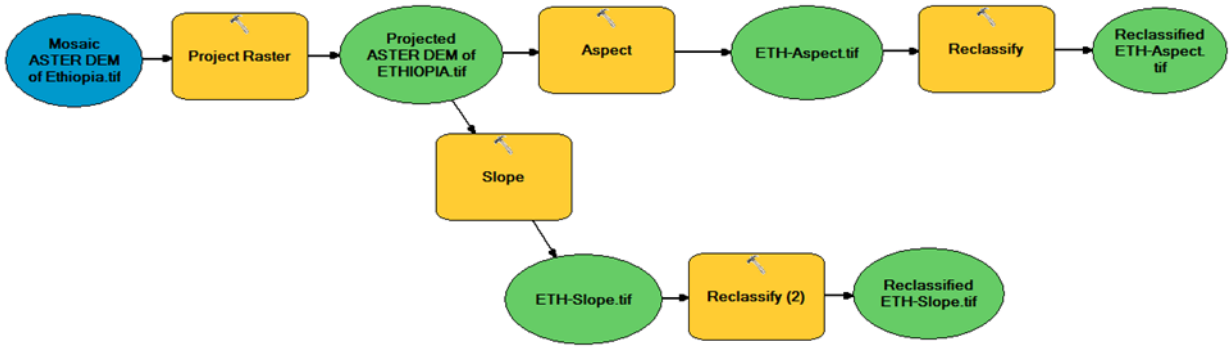

GIS Model to Convert Land Cover and Population Density Polygons to Raster and to Project and Reclassify the output Raster into Five Suitability Level

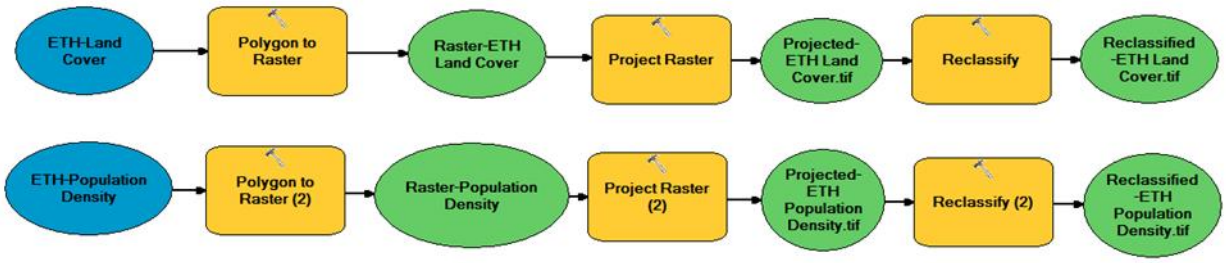

GIS Model to Create Fuzzy Membership Raster of each Criterion and to obtain Suitability Map for large-scale PV installations in Ethiopia using Weighted Sum tool

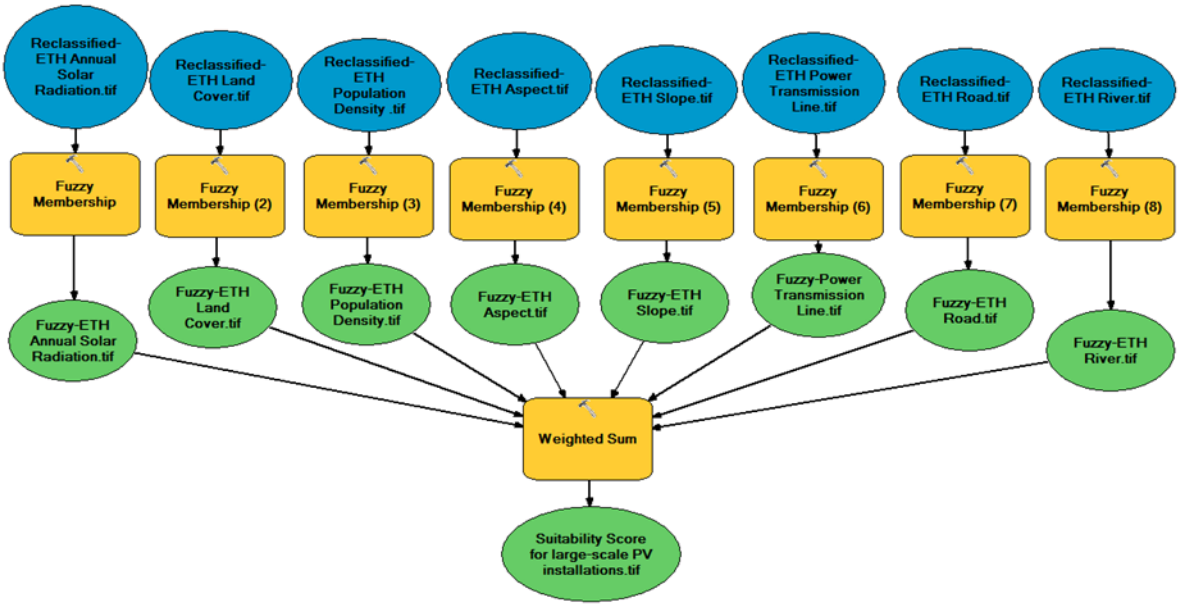

GIS Model to convert Suitability Score Raster to Polygons

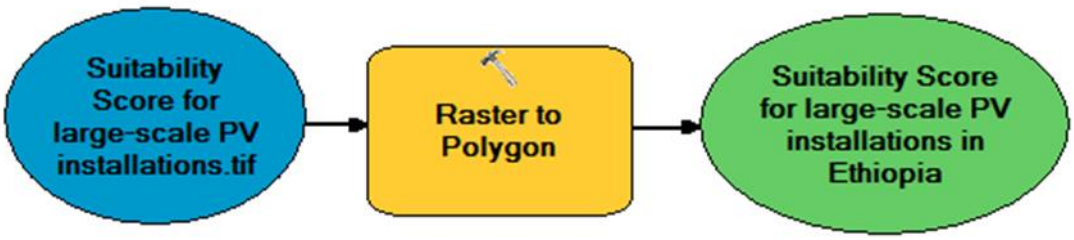

Small polygons less than 2.5 km^2 were filtered out using Selection by Attributes. Finally, 195 Ideal Sites (Polygons) with aggregate capacity of 500 TWh/year were selected for large-scale PV installations in Ethiopia.

Appendix D: Locations and Characteristics of the Selected Sites for Large-Scale PV Installations in Ethiopia

ID	X-Coordinate (m)	Y-Coordinate (m)	Woreda	Zone	Region	Area-km^2	EGP (Twh/year)
1	536436	1477309	Hintalo Wajirat	South Tigray	Tigray	21.8	2.1
2	503066	1456858	Abergele	Wag Himra	Amhara	11.2	1.1
2			Tanqua Abergele	Central Tigray	Tigray		0.0
3	634762	1344975	Awura	Zone 04	Afar	21.5	2.1
4	826938	1322921	Elidar	Zone 01	Afar	14.3	1.4
5	792357	1327212	Elidar	Zone 01	Afar	92.3	8.9
6	607448	1328821	Awura	Zone 04	Afar	120.5	11.6
7	647558	1322364	Awura	Zone 04	Afar	11.8	1.1
8	659415	1302222	Dubti	Zone 01	Afar	14.3	1.4
9	795609	1289915	Elidar	Zone 01	Afar	11.8	1.1
10	692223	1283279	Mile	Zone 01	Afar	15.8	1.5
11	685610	1280218	Mile	Zone 01	Afar	16.0	1.5
12	671381	1277399	Mile	Zone 01	Afar	5.9	0.6
13	681384	1274595	Mile	Zone 01	Afar	36.7	3.5
14	639986	1268937	Adear	Zone 01	Afar	16.9	1.6
15	644446	1264739	Adear	Zone 02	Afar	20.1	1.9
16	633621	1263436	Adear	Zone 03	Afar	41.0	4.0
17	652465	1257195	Adear	Zone 04	Afar	113.1	10.9
18	661425	1244669	Adear	Zone 05	Afar	6.7	0.6
19	655243	1244008	Adear	Zone 06	Afar	2.5	0.2
20	650907	1233914	Telalak	Zone 05	Afar	71.1	6.9
20			Adear	Zone 07			0.0
21	725008	1225961	Erer	Shinile	Somali	2.7	0.3
22	647790	1224731	Telalak	Zone 05	Afar	21.9	2.1
23	722650	1221251	Erer	Shinile	Somali	26.9	2.6
24	722347	1213971	Erer	Shinile	Somali	12.2	1.2
25	649158	1213023	Talalak	Zone 05	Afar	37.3	3.6
26	726291	1208625	Erer	Shinile	Somali	12.8	1.2
27	724352	1206100	Erer	Shinile	Somali	2.8	0.3
28	648997	1202193	Telalak	Zone 05	Afar	48.2	4.6
29	890558	1197066	Ayisha	Shinile	Somali	11.5	1.1
30	697492	1197681	Erer	Shinile	Somali	12.0	1.2
31	677181	1204628	Erer	Shinile	Somali	72.7	7.0
32	707685	1187773	Erer	Shinile	Somali	23.1	2.2
33	672648	1190763	Erer	Shinile	Somali	60.6	5.8

ID	X-Coordinate (m)	Y-Coordinate (m)	Woreda	Zone	Region	Area-km^2	EGP (Twh/year)
34	873065	1186178	Ayisha	Shinile	Somali	55.0	5.3
35	899872	1183570	Ayisha	Shinile	Somali	15.8	1.5
36	894081	1182583	Ayisha	Shinile	Somali	23.3	2.2
37	887797	1183402	Ayisha	Shinile	Somali	28.4	2.7
38	819719	1171309	Ayisha	Shinile	Somali	19.2	1.9
39	714636	1174558	Erer	Shinile	Somali	47.6	4.6
40	838207	1167780	Ayisha	Shinile	Somali	24.0	2.3
41	848279	1164871	Ayisha	Shinile	Somali	12.3	1.2
42	887814	1167702	Ayisha	Shinile	Somali	34.8	3.4
43	642063	1157424	Hadeleala	Zone 05	Afar	26.8	2.6
44	736127	1156292	Erer	Shinile	Somali	34.8	3.4
45	821787	1156472	Ayisha	Shinile	Somali	32.0	3.1
46	742632	1154335	Shinile	Shinile	Somali	15.4	1.5
47	835908	1152384	Ayisha	Shinile	Somali	12.4	1.2
48	785076	1152967	Shinile	Shinile	Somali	23.5	2.3
49	873357	1149013	Ayisha	Shinile	Somali	6.1	0.6
50	832818	1157162	Ayisha	Shinile	Somali	62.4	6.0
51	641038	1150522	Hadeleala	Zone 05	Afar	56.9	5.5
52	771181	1148298	Shinile	Shinile	Somali	64.0	6.2
53	688041	1140149	Erer	Shinile	Somali	7.5	0.7
54	704273	1140978	Erer	Shinile	Somali	11.4	1.1
55	843460	1136945	Ayisha	Shinile	Somali	12.1	1.2
55	843460	1136945	Shinile	Shinile	Somali	12.1	1.2
56	812674	1135912	Shinile	Shinile	Somali	11.6	1.1
57	823172	1135714	Shinile	Shinile	Somali	87.9	8.5
58	903282	1128441	Ayisha	Shinile	Somali	22.6	2.2
59	700483	1126070	Erer	Shinile	Somali	19.3	1.9
60	836810	1126114	Shinile	Shinile	Somali	15.8	1.5
61	696511	1120570	Erer	Shinile	Somali	14.4	1.4
62	817736	1122159	Shinile	Shinile	Somali	26.2	2.5
63	648088	1119207	Hadeleala	Zone 05	Afar	21.0	2.0
64	733351	1118157	Erer	Shinile	Somali	27.3	2.6
65	18867	1114785	Assosa	Assosa	Beneshangul	31.5	3.0
66	867722	1112529	Denbel	Shinile	Somali	22.5	2.2
67	12903	1107944	Assosa	Assosa	Beneshangul	11.8	1.1
68	23737	1109620	Assosa	Assosa	Beneshangul	35.6	3.4
69	642213	1104789	Semurobina Gelalo	Zone 05	Afar	50.2	4.8
70	10841	1102488	Assosa	Assosa	Beneshangul	29.3	2.8

ID	X-Coordinate (m)	Y-Coordinate (m)	Woreda	Zone	Region	Area-km^2	EGP (Twh/year)
71	682122	1101533	Afdem	Shinile	Somali	91.0	8.8
72	29431	1096072	Bambasi	Assosa	Beneshangul	29.4	2.8
73	883682	1092090	Denbel	Shinile	Somali	11.0	1.1
74	674097	1091898	Afdem	Shinile	Somali	10.9	1.0
75	873436	1091105	Denbel	Shinile	Somali	36.4	3.5
76	24441	1089619	Bambasi	Assosa	Beneshangul	26.1	2.5
77	678460	1087839	Afdem	Shinile	Somali	37.6	3.6
78	947738	1089690	Awubere	Jijiga	Somali	105.6	10.2
79	825067	1078226	Shinile	Shinile	Somali	13.3	1.3
80	905566	1077799	Denbel	Shinile	Somali	21.8	2.1
81	33773	1075058	Bambasi	Assosa	Beneshangul	19.4	1.9
82	339121	1077326	Hababo Guduru	Horo Gidru Wellega	Oromia	33.3	3.2
83	961243	1074366	Awubere	Jijiga	Somali	30.9	3.0
84	936195	1072423	Awubere	Jijiga	Somali	27.3	2.6
85	788855	1074021	Erer	Shinile	Somali	49.4	4.8
85			Shinile				0.0
86	338732	1068188	Hababo Guduru	Horo Gidru Wellega	Oromia	14.9	1.4
87	697771	1065031	Afdem	Shinile	Somali	13.0	1.3
88	690667	1070166	Afdem	Shinile	Somali	119.1	11.5
89	624269	1060374	Dulecha	Zone 03	Afar	31.7	3.1
90	337757	1060746	Gudru	Horo Gidru Wellega	Oromia	15.0	1.4
90			Hababo Guduru				0.0
91	955871	1062175	Awubere	Jijiga	Somali	214.8	20.7
92	971043	1056303	Awubere	Jijiga	Somali	16.6	1.6
93	713123	1053776	Afdem	Shinile	Somali	17.0	1.6
94	719450	1060303	Afdem	Shinile	Somali	137.6	13.3
95	619403	1053929	Dulecha	Zone 03	Afar	99.7	9.6
96	332530	1042801	Guduru	Horo Gidru Wellega	Oromia	41.0	4.0
97	1000191	1030430	Kebri Beyah	Jijiga	Somali	11.6	1.1
98	310969	1029476	Guduru	Horo Gidru Wellega	Oromia	13.0	1.3
98			Jima Rare				0.0
99	614435	1039696	Dulecha	Zone 03	Afar	82.2	7.9
100	606513	1019058	Awash Fentale	Zone 03	Afar	14.3	1.4
101	601719	1015581	Awash Fentale	Zone 03	Afar	15.5	1.5
102	1031222	1012529	Harshin	Jijiga	Somali	59.2	5.7
103	614645	1011450	Awash Fentale	Zone 03	Afar	23.6	2.3
104	623377	1008049	Awash Fentale	Zone 03	Afar	66.3	6.4
105	1019318	997213	Harshin	Jijiga	Somali	38.7	3.7

ID	X-Coordinate (m)	Y-Coordinate (m)	Woreda	Zone	Region	Area-km^2	EGP (Twh/year)
106	1005885	994087	Harshin	Jijiga	Somali	14.4	1.4
107	1062450	989750	Harshin	Jijiga	Somali	12.5	1.2
108	1066128	985031	Harshin	Jijiga	Somali	13.0	1.3
109	1003434	984785	Harshin	Jijiga	Somali	23.2	2.2
110	535053	982213	Minjar Shenkora	North Shewa	Amhara	7.8	0.8
111	773980	977415	Gole Oda	East Harerge	Oromia	29.8	2.9
112	1003150	971445	Degehabur	Degehabur	Somali	27.6	2.7
113	554593	968343	Minjar Shenkora	North Shewa	Amhara	19.5	1.9
114	985616	969534	Degehabur	Degehabur	Somali	89.2	8.6
115	1010020	956071	Degehabur	Degehabur	Somali	16.7	1.6
116	986920	954504	Degehabur	Degehabur	Somali	45.4	4.4
117	752861	933311	Gole Oda	East Harerge	Oromia	11.7	1.1
118	1013021	930338	Degehabur	Degehabur	Somali	3.9	0.4
119	710601	871107	Legehida	Bale	Oromia	13.9	1.3
120	597352	866791	Amigna	Arsi	Oromia	31.3	3.0
121	607666	865588	Amigna	Arsi	Oromia	8.8	0.8
122	595219	858135	Amigna	Arsi	Oromia	35.2	3.4
123	729515	837681	Seweyna	Bale	Oromia	13.3	1.3
124	111530	822861	Bita	Kefa	SNNP	6.2	0.6
125	722553	822450	Seweyna	Bale	Oromia	18.0	1.7
126	642859	815568	Gasera	Bale	Oromia	5.7	0.6
127	741390	812313	Seweyna	Bale	Oromia	10.2	1.0
128	88104	813286	Mengesh	Mejenger	Gambella	24.0	2.3
129	651764	812139	Gololcha	Bale	Oromia	16.9	1.6
130	697855	809550	Seweyna	Bale	Oromia	3.1	0.3
131	651266	805285	Ginir	Bale	Oromia	11.4	1.1
132	704580	800345	Seweyna	Bale	Oromia	19.3	1.9
133	652679	796021	Ginir	Bale	Oromia	43.3	4.2
134	1076063	790539	Kebridehar	Korahe	Somali	10.2	1.0
135	551265	786874	Adaba	West Arsi	Oromia	28.1	2.7
136	537852	782536	Adaba	West Arsi	Oromia	11.7	1.1
137	726568	781940	Raitu	Bale	Oromia	11.1	1.1
138	601572	778509	Goba	Bale	Oromia	3.1	0.3
139	545005	780636	Adaba	West Arsi	Oromia	47.8	4.6
140	604714	775416	Goba	Bale	Oromia	11.4	1.1
141	1070739	776444	Kebridehar	Korahe	Somali	21.0	2.0
142	567114	771253	Adaba	West Arsi	Oromia	12.4	1.2
143	617257	775155	Goba	Bale	Oromia	46.5	4.5

ID	X-Coordinate (m)	Y-Coordinate (m)	Woreda	Zone	Region	Area-km^2	EGP (Twh/year)
144	644198	772508	Goro	Bale	Oromia	30.8	3.0
145	595906	767388	Goba	Bale	Oromia	37.8	3.7
146	604978	761894	Goba	Bale	Oromia	17.2	1.7
147	577597	760891	Adaba	West Arsi	Oromia	37.8	3.6
148	802535	757662	Raitu	Bale	Oromia	10.7	1.0
149	602804	752336	Goba	Bale	Oromia	11.4	1.1
150	580043	752525	Goba	Bale	Oromia	42.8	4.1
151	589541	744951	Goba	Bale	Oromia	20.7	2.0
152	189085	663569	Selamago	South Omo	SNNP	15.8	1.5
153	183807	647818	Selamago	South Omo	SNNP	13.6	1.3
154	544168	631409	Liben	Guji	Oromia	26.8	2.6
155	543986	623516	Liben	Guji	Oromia	34.3	3.3
156	550071	612588	Liben	Guji	Oromia	21.7	2.1
157	547568	607333	Liben	Guji	Oromia	22.1	2.1
158	561235	603308	Liben	Guji	Oromia	114.1	11.0
159	550248	595376	Liben	Guji	Oromia	127.2	12.3
160	179763	588442	Gnangatom	South Omo	SNNP	18.7	1.8
161	170445	586177	Gnangatom	South Omo	SNNP	14.7	1.4
162	409745	584949	Yabelo	Borena	Oromia	16.6	1.6
163	552710	585214	Liben	Guji	Oromia	36.6	3.5
164	537096	587240	Liben	Guji	Oromia	50.5	4.9
165	245872	577274	Hamer	South Omo	SNNP	10.6	1.0
166	418283	579452	Yabelo	Borena	Oromia	16.3	1.6
167	623884	577507	Filtu	Liben	Somali	26.0	2.5
168	396343	576484	Yabelo	Borena	Oromia	12.0	1.2
169	425808	573195	Yabelo	Borena	Oromia	14.0	1.3
170	434895	568440	Yabelo	Borena	Oromia	14.6	1.4
171	669395	564587	Filtu	Liben	Somali	12.8	1.2
172	441415	563269	Yabelo	Borena	Oromia	20.4	2.0
173	603949	560081	Filtu	Liben	Somali	11.6	1.1
174	424774	552994	Yabelo	Borena	Oromia	12.5	1.2
175	431927	558727	Yabelo	Borena	Oromia	132.8	12.8
176	428523	548938	Yabelo	Borena	Oromia	14.3	1.4
177	423767	548525	Yabelo	Borena	Oromia	5.6	0.5
178	449580	549389	Arero	Borena	Oromia	20.9	2.0
179	479336	541791	Arero	Borena	Oromia	26.0	2.5
180	347517	536717	Teltele	Borena	Oromia	12.0	1.2
181	428347	534962	Yabelo	Borena	Oromia	12.4	1.2

ID	X-Coordinate (m)	Y-Coordinate (m)	Woreda	Zone	Region	Area-km^2	EGP (Twh/year)
182	265637	535639	Hamer	South Omo	SNNP	22.0	2.1
183	440281	532829	Arero	Borena	Oromia	12.2	1.2
183	440281	532829	Yabelo	Borena	Oromia	12.2	1.2
184	437854	527742	Arero	Borena	Oromia	15.4	1.5
184	420028	529872	Yabelo	Borena	Oromia	10.5	1.0
185	437854	527742	Yabelo	Borena	Oromia	15.4	1.5
186	426299	524363	Yabelo	Borena	Oromia	16.9	1.6
187	255416	519456	Teltele	Borena	Oromia	4.0	0.4
188	246432	514044	Teltele	Borena	Oromia	20.3	2.0
189	448901	503338	Arero	Borena	Oromia	11.7	1.1
190	422129	505634	Dire	Borena	Oromia	46.2	4.5
191	428838	501670	Dire	Borena	Oromia	19.4	1.9
192	436833	499924	Arero	Borena	Oromia	57.4	5.5
192	436833	499924	Dire	Borena	Oromia	57.4	5.5
193	450656	497255	Arero	Borena	Oromia	28.2	2.7
194	431529	482746	Dire	Borena	Oromia	5.5	0.5
195	311149	477451	Teltele	Borena	Oromia	46.7	4.5